



Published in final edited form as:

Cell. 2018 May 17; 173(5): 1265–1279.e19. doi:10.1016/j.cell.2018.03.037.

## The neuropeptide Tac2 controls a distributed brain state induced by chronic social isolation stress

Moriel Zelikowsky<sup>1,\*</sup>, May Hui<sup>1</sup>, Tomomi Karigo<sup>1</sup>, Andrea Choe<sup>1</sup>, Bin Yang<sup>1</sup>, Mario Blanco<sup>1</sup>, Keith Beadle<sup>1</sup>, Viviana Gradinaru<sup>1</sup>, Benjamin E. Deverman<sup>1</sup>, and David J. Anderson<sup>1,2,3,4,\*</sup>

<sup>1</sup>Division of Biology and Biological Engineering 156-29, California Institute of Technology Pasadena, CA 91125, USA

<sup>2</sup>Howard Hughes Medical Institute, California Institute of Technology Pasadena, CA 91125, USA

<sup>3</sup>Tianqiao and Chrissy Chen Institute for Neuroscience, California Institute of Technology Pasadena, CA 91125, USA

### Abstract

Chronic social isolation causes severe psychological effects in humans, but their neural bases remains poorly understood. Two weeks (but not 24 hrs) of social isolation stress (SIS) caused multiple behavioral changes in mice, and induced brain-wide up-regulation of the neuropeptide tachykinin 2 (Tac2)/neurokinin B (NkB). Systemic administration of an Nk3R antagonist prevented virtually all of the behavioral effects of chronic SIS. Conversely, enhancing NkB expression and release phenocopied SIS in group-housed mice, promoting aggression and converting stimulus-locked defensive behaviors to persistent responses. Multiplexed analysis of Tac2/NkB function in multiple brain areas revealed dissociable, region-specific requirements for both the peptide and its receptor in different SIS-induced behavioral changes. Thus, Tac2 coordinates a pleiotropic brain state caused by SIS, via a distributed mode of action. These data reveal the profound effects of prolonged social isolation on brain chemistry and function, and suggest potential new therapeutic applications for Nk3R antagonists.

\*Correspondence: moriel@caltech.edu (M.Z.), wuwei@caltech.edu (D.J.A.).

<sup>4</sup>Lead Contact

### DECLARATION OF INTERESTS

The authors declare no competing interests. B.E.D. and V.G. are listed as inventors on a patent related to AAV-PHP.B (#US9585971B2).

### SUPPLEMENTAL INFORMATION

Supplemental Information includes seven figures and two tables and can be found with this article online.

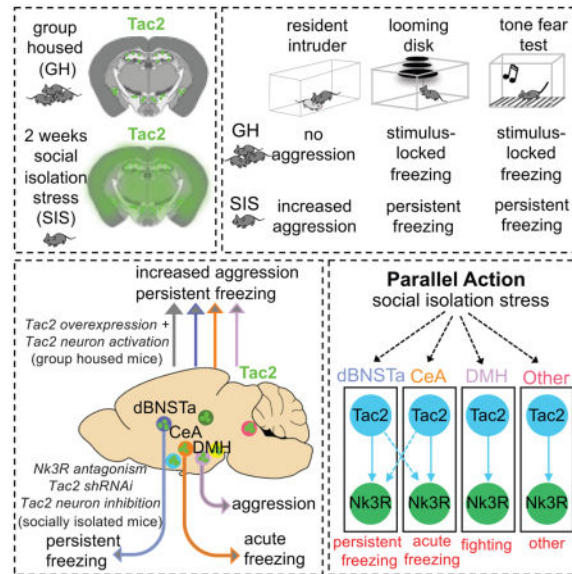
### AUTHOR CONTRIBUTIONS

M.Z. and D.J.A. contributed to the study design. M.Z., M.H., A.C., M.B. and B.D. contributed to the data collection, scoring and analysis. M.Z. and M.H. conducted the surgeries, behavior experiments, and histological analyses. K.B. performed PHP.B viral packaging and B.E.D. helped design PHP.B experiments and performed retro-orbital viral injections. T.K. contributed the shRNA and Tac2 cDNA constructs. B.Y. contributed to packaging of viral constructs. M.B. contributed to qRT-PCR analyses. V.G. provided funding to support K.B. and B.E.D. and comments on manuscript. M.Z. and D.J.A. wrote the paper. All authors discussed and commented on the manuscript.

**Publisher's Disclaimer:** This is a PDF file of an unedited manuscript that has been accepted for publication. As a service to our customers we are providing this early version of the manuscript. The manuscript will undergo copyediting, typesetting, and review of the resulting proof before it is published in its final citable form. Please note that during the production process errors may be discovered which could affect the content, and all legal disclaimers that apply to the journal pertain.

## Graphical Abstract

The Tac2 neuropeptide system orchestrates the complex behavioral effects of chronic social isolation stress by acting locally in multiple brain regions, suggesting the therapeutic potential of Nk3R antagonists for managing behavioral changes upon prolonged social isolation.



## Keywords

Tac2; neuropeptides; social isolation; stress; aggression; fear

## INTRODUCTION

Internal states of arousal, motivation and emotion exert a major influence on how the brain processes sensory information to control behavior (Berridge, 2004; Bargmann, 2012; LeDoux, 2012; Anderson and Adolphs, 2014; Anderson, 2016). An important class of internal states is that produced by exposure to psychogenic stressors (McEwen *et al.*, 2015). Chronic stress in particular has profound, long-lasting effects on both physical and mental health (Selye, 1936; House *et al.*, 1988; Sapolsky, 1996; Cacioppo and Hawkley, 2009; Kessler *et al.*, 2009; Holt-Lunstad *et al.*, 2010; Cacioppo *et al.*, 2014; Holt-Lunstad *et al.*, 2015). However, most animal models of chronic stress entail repeated administration of acute stressors, and hence contain within them a reprieve from the stressor (Katz *et al.*, 1981). Thus, although the stress is repeatedly administered, it is intermittent.

Chronic social isolation stress (SIS) provides one of the few paradigms in which a stressor can be applied continuously for extended periods (days or weeks) (Hilakivi *et al.*, 1989; Weiss *et al.*, 2004). Social isolation stress is widespread in humans and has detrimental effects on health (House *et al.*, 1988). However its neurobiological basis remains poorly understood. For example, there is conflicting evidence on whether or not prolonged SIS chronically activates the HPA axis (Hawkley *et al.*, 2012; Cacioppo *et al.*, 2015). A recent study implicated dorsal raphe dopaminergic neurons in mediating effects of relatively brief

(24 hr) social isolation in mice (Matthews *et al.*, 2016), but a subsequent study described a broader role for these neurons in promoting arousal (Cho *et al.*, 2017).

Neuropeptides, most notably CRH, have been implicated in mediating stress responses in a variety of systems (reviewed in Kormos and Gaszner, 2013; Witkin *et al.*, 2014; Kash *et al.*, 2015; Chen, 2016), but the logic underlying their actions is not yet clear (Fig. 1A–D). Guided by our previous studies of aggression in *Drosophila* (Wang *et al.*, 2008; Asahina *et al.*, 2014), we have investigated a potential role for tachykinins in mediating social isolation stress (SIS)-induced aggression in mice (Maggio, 1988). Studies of Tac2/NkB in the central amygdala have implicated the peptide in fear memory consolidation (Andero *et al.*, 2014; Andero *et al.*, 2016), suggesting a role in fear learning and expression. Here we report a broader and unanticipated role for Tac2/NkB as an important peptide mediator of the effects of chronic SIS. Tac2/NkB is dramatically up-regulated by SIS throughout the brain, and coordinates a pervasive change in brain state, affecting not only aggression but many other behaviors, via distributed local actions in multiple brain regions.

## RESULTS

### Chronic social isolation stress produces widespread effects on multiple defensive behaviors

Prolonged SIS is known to promote multiple behavioral effects, including increased aggression and persistent responses to threats, in both humans and animal models (Hatch *et al.*, 1963; Valzelli, 1969, 1973; Weiss *et al.*, 2004; Matsumoto *et al.*, 2005; Arrigo and Bullock, 2008; An *et al.*, 2017). As an initial step, therefore, we examined the effects of 2 weeks of SIS in wildtype C57Bl6/N mice using multiple behavioral assays: aggression in the resident-intruder (RI) assay (Thurmond, 1975), innate freezing to an overhead looming disk (LD) (Yilmaz and Meister, 2013), learned freezing to a conditioned tone (2.8 kHz) (Fanselow, 1980), and reactivity to a footshock (0.7mA) (Fig. 1E–I and S1B–D). SIS produced a robust increase in offensive aggression towards a submissive intruder, compared to non-aggressive group housed controls (Fig. 1F), confirming previous studies (Valzelli, 1969; Matsumoto *et al.*, 2005; Toth *et al.*, 2011). It also caused persistent freezing to both the LD and CS (Fig. 1G, H, *post*, red bars), in contrast to GH controls where freezing terminated with stimulus offset. However the magnitude of freezing to both the overhead LD and the conditioned tone was unaffected by SIS (Fig. 1G, H, *during*), as was the rate and asymptotic value of conditioned fear acquisition (Fig. S1A). SIS mice also showed significantly enhanced reactivity to a footshock (Fig. 1I), increased freezing to a threatening ultrasonic stimulus (USS) (Mongeau *et al.*, 2003) (Fig. 1J–K), increased tail rattling to the LD (Fig. S1E), increased sensitivity to sub-threshold acoustic startle stimuli (Fig. S1I), and a decreased latency to flinch to a mild footshock (Fig. S1H).

SIS mice were also tested for anxiety-like behavior in the open field test (OFT) and the elevated plus maze (EPM) (Figs. 1L–N, S1F). They showed a modest but significant reduction in time spent in the center of the OFT arena, without a change in velocity (Fig. 1M), but were no different from GH mice on the EPM test (Fig. 1N). However, SIS mice showed an increased propensity to jump off the EPM platform (Fig. S1F). Lastly, SIS mice spent less time interacting with a novel mouse in a social interaction assay (although their

latency to initially approach the mouse was reduced; Fig. S1J) but more time closer to a predator (rat) (Fig. S1G). Collectively, these findings demonstrate that SIS alters behavioral responses to a variety of stimuli (summarized in Fig. 1O). This profile appears different from anxiety (Blanchard *et al.*, 2003; Bourin *et al.*, 2007), consistent with earlier studies in mice (Hilakivi *et al.*, 1989). Importantly, when we isolated mice for just 24 hr, we failed to detect any of the behavioral alterations we observed following 2 weeks of SIS (Fig. S3A–E), distinguishing this paradigm from the effects of short-term SI studied previously (Matthews *et al.*, 2016).

### Chronic SIS causes widespread up-regulation of *Tac2* transcription

In *Drosophila*, an unbiased screen of peptidergic neurons identified DTK (*Drosophila* tachykinin)-expressing neurons, and the DTK peptide, as required for social isolation-induced aggression (Asahina *et al.*, 2014). To determine whether this function might be conserved, we investigated the role of tachykinins in SIS. In rodents, the tachykinin gene family comprises *Tac1* and *Tac2* (Maggio, 1988). *Tac1* encodes the peptides substance P (SP), as well as neurokinin A (NkA); *Tac2* encodes neurokinin B (NkB). These peptides bind with the highest affinities to the G-protein coupled Nk1, Nk2, and Nk3 receptors, respectively (Fig. 2A) (Ebner *et al.*, 2009). *Tac1* and *Tac2* are expressed in a variety of brain regions implicated in emotion and social behavior (Fig. 2B) (Culman and Unger, 1995).

To determine whether *Tac* gene expression is influenced by SIS, we crossed *Tac2-IRES-Cre* or *Tac1-IRES-Cre* knock-in mice (Tasic *et al.*, 2016) to a Cre-reporter mouse (line Ai6) expressing zsGreen (Madisen *et al.*, 2010). Double-heterozygous mice were socially isolated for two weeks or group housed prior to sacrifice. Strikingly, freshly dissected brains from isolated *Tac2-Cre; Ai6* (but not *Tac1-Cre; Ai6*) mice exhibited enhanced cortical reporter expression that could be detected by the naked eye under ambient lighting (Fig. S2A). Histology confirmed a widespread increase in zsGreen expression, in both males (Fig. 2C; S2B) and females (Fig. S2C). Up-regulation was evident in the anterior dorsal bed nucleus of the stria terminalis (dBNSTa), central nucleus of the amygdala (CeA), dorsomedial hypothalamus (DMH), as well as the cortex and striatum (Fig. S2A, B). Cell-specific markers indicated that most zsGreen expression occurred in neuronal cells (Fig. S2D). Increased zsGreen expression was also detected in peripheral endocrine tissues, such as the pancreas, testes and submandibular gland (not shown).

Similar results were obtained using a different Cre reporter mouse, Ai14 (Madisen *et al.*, 2010) expressing tdTomato (Fig. S2E), indicating that the induction was not a peculiarity of the Ai6 line. Importantly, no such change was observed in SIS *Tac1-Cre; Ai6* mice (Figs. 2D; S2A). These data suggest that the induction of zsGreen observed in SIS mice is specific to the *Tac2<sup>Cre</sup>* allele, and is not a non-specific effect of SIS to increase Cre-mediated recombination at the *Rosa-26* locus, or a peculiarity of the zsGreen reporter.

To confirm that SIS up-regulated endogenous *Tac2* expression, we quantified *Tac2* mRNA in selected brain regions using qRT-PCR and RNA fluorescent in situ hybridization (FISH). QRT-PCR indicated that SIS caused a large (~3–8 –fold) and significant increase in *Tac2* mRNA levels in the dBNSTa, DMH and CeA, with trends to an increase in the ACC and dHPC (Fig. 2E). An increase in NkB protein expression was also observed in these regions

by immunostaining (Fig. S2I). A time-course revealed a gradual increase in Tac2 mRNA from 30 min to 2 weeks of SIS (Fig. S2F). No increase in Tac1 mRNA was observed following SIS (Fig. 2F, S2G).

Endogenous Tac2 mRNA up-regulation was also observed by FISH in in dBNSTa, CeA and DMH (Figs. 2G–P). Up-regulation in CeA was significant in both its medial and lateral subdivisions (Kim *et al.*, 2017). The fold-increase in fluorescence intensity per mm<sup>2</sup> was much greater than the fold-increase in the number of Tac2 mRNA<sup>+</sup> cells (Fig. 2L–P). In contrast, the Cre reporter transgene, which integrates and amplifies changes in expression, yielded a larger fold-increase in the number of positive cells (Fig. S2B). This difference was particularly evident in the ACC or dHPC (Fig. 2J–K, O–P and Fig. S2B), suggesting amplification of induction by the Cre reporter. Despite these quantitative differences, the mRNA data confirm that SIS up-regulates endogenous Tac2 expression in multiple brain regions.

### Acute systemic antagonism of Nk3Rs attenuates the effects of SIS

To investigate a causal role for NkB in mediating behavioral effects of SIS, we systemically administered osanetant (Fig. 3A) (Emonds-Alt *et al.*, 1995), a specific Nk3R antagonist that crosses the blood-brain barrier (Spooren *et al.*, 2005). Osanetant delivered after SIS, but 20 min prior to each test, strongly reduced aggression enhanced by SIS (Fig. 3B), but not by sexual experience (Remedios *et al.*, 2017) (Fig. S3J–K). It also attenuated persistent freezing to both the LD and the fear-conditioned tone (Fig. 3C, D, *post*, green bars), but not acute freezing during stimulus presentation. Osanetant also attenuated other SIS-induced behaviors including increased shock reactivity (Fig. 3E), increased tail-rattling (Fig. S3G), decreased social interaction (Fig. S3H) and enhanced responding in the acoustic startle assay (Fig. S3I). Thus, systemic antagonism of Nk3Rs blocked virtually all of the measured behavioral effects of chronic SIS, while leaving non-SIS altered behaviors intact (Fig. S3K). Notably, osanetant also blocked persistent freezing to the LD caused by prior footshock (Fig. S3L–M), suggesting involvement of NkB in responses to other stressors.

### Chronic systemic antagonism of Nk3Rs during SIS has a protective effect

To investigate whether Tac2 signaling is required during SIS, mice were administered osanetant daily in their home cage during the two-week isolation period, but were then tested off-drug. To control for carry-over of the drug from the last home-cage administration into the testing period (24 hrs later), an additional group of SIS mice was given a single home-cage administration of osanetant 24 hours prior to testing (Fig. 3F).

Treatment with daily osanetant prevented SIS-enhanced aggression (Fig. 3G), persistent freezing to the LD (Fig. 3H), and persistent freezing to the fear conditioned tone (Fig. 3I). The SIS-induced increase in shock reactivity was reduced, but not significantly (Fig. 3J, K). Strikingly, mice that had been treated with osanetant during SIS could be returned to housing with their pre-isolation cagemates without any subsequent fighting observed, in contrast to control SIS mice which vigorously attacked their cagemates when reintroduced to the group (data not shown).

### Nk3Rs act in different brain regions to mediate effects of SIS on different behaviors

We next asked where in the brain NkB signaling is required to mediate the behavioral effects of SIS. The dBNSTa, DMH, and CeA exhibited strong induction of Tac2 by SIS (Fig. 2), and also contain cells expressing Nk3Rs (Fig. S4A). Since Tac2<sup>+</sup> neurons in CeA and dBNSTa project to multiple distal targets (Fig. S4B–D; Table S2), as a first step, we pharmacologically inhibited Nk3Rs locally in these Tac2-expressing regions. SIS mice received bilateral microinfusions of osanetant into a given region 20 minutes prior to each behavioral test (Fig. 4A). We selected four assays – the RI assay, LD, fear conditioning, and shock reactivity – because they exhibited robust SIS-induced changes and could be performed sequentially within the same animals without affecting each other (as indicated by initial experiments in which the assays performed following aggression testing were performed independently, Fig. S1C–D).

Local infusion of osanetant in dBNSTa selectively inhibited persistent, but not acute, freezing to both the LD and the conditioned tone (Figs. 4C–D), but had no effect on aggression (Fig. 4B) or shock reactivity (Fig. S4F). By contrast, osanetant microinfused into the DMH abolished aggression (Fig. 4E), but had no effect on persistent responses to the LD (Fig. 4F) or the conditioned tone (Fig. 4G), or on footshock reactivity (Fig. S4G). (However, DMH-infused mice showed an increase in the latency to first orient and freeze to the LD; Fig. S4E). Lastly, osanetant infusion into the CeA reduced acute (and thereby persistent) freezing to the innate and conditioned threatening stimuli, as well as reactivity to the footshock (Figs. 4H–K, S4H), but not aggression. Infusion of osanetant into the ACC or striatum failed to yield significant effects on SIS-induced persistent freezing to the LD (Figs. S4I–J).

### Region-specific chemogenetic silencing of Tac2<sup>+</sup> neurons blocks distinct behavioral responses to SIS

To determine whether Tac2 up-regulation in dBNSTa, DMH and CeA reflected a requirement for NkB release in these structures, we first asked whether the activity of Tac2<sup>+</sup> neurons in these regions was required for the effects of SIS. Tac2/c-fos dFISH experiments revealed a significant induction of c-fos in Tac2<sup>+</sup> cells in dBNSTa and CeA following exposure to the LD or conditioned tone, but not during aggression. Conversely, Tac2<sup>+</sup> cells in DMH were activated during aggression but not during threat exposure (Fig S5A–D).

To determine whether silencing Tac2<sup>+</sup> cells could prevent the effects of SIS, Tac2-IRES-Cre mice were bilaterally injected in dBNSTa, CeA or DMH with a Cre-dependent AAV encoding hM4DREADD (AAV2-DIO-hM4D-mCherry) (Conklin *et al.*, 2008). Following 3 weeks to allow viral expression (Fig. S5E) and 2 weeks of SIS, mice were tested for SIS-induced behavioral changes 20 minutes after injection of clozapine-N-oxide (CNO) or vehicle (Fig. 5A).

Chemogenetic silencing of Tac2<sup>+</sup> cells in dBNSTa, DMH, and CeA essentially phenocopied the effect of local osanetant infusions. In dBNSTa, persistent freezing responses were selectively attenuated (Figs. 5B–D, *post*), while in DMH aggression was inhibited (Figs. 5E–G), and in CeA acute freezing and shock reactivity were suppressed (Figs. 5H–K, S5H). No

effects of CNO were observed in control mice subjected to the same series of behavioral assays (Fig. 5SI–N), excluding off-target effects (Gomez *et al.*, 2017). Thus the activity of Tac2<sup>+</sup> neurons, like Nk3R function, is differentially required in different brain regions for different behavioral effects of SIS.

### Tac2 synthesis is differentially required in dBNSTa, CeA, and DMH

We asked next whether Tac2 synthesis was required in each of the three brain regions studied, via targeted shRNAi-mediated knockdown of Tac2. Mice were injected stereotaxically in dBNSTa, DMH, or CeA with adeno-associated viruses (AAVs) expressing small hairpin RNAs (shRNAs), together with a CMV promoter-driven zsGreen fluorescent reporter (AAV5-H1-shRNA-CMV-zsGreen). Two shRNAs (shRNA-1 and shRNA-2) proved effective as determined by FISH and qRT-PCR, with shRNA-2 yielding the strongest reductions in Tac2 mRNA (Fig. S6E–G). Control mice were injected with an AAV encoding an shRNA targeted to the *luciferase* gene. Injections were histologically verified by zsGreen fluorescence. The number of zsGreen<sup>+</sup> neurons was not significantly different between animals injected with control vs. experimental shRNA's, suggesting that the reduction in the number of Tac2 mRNA<sup>+</sup> cells was not due to cell death (Fig. S6D).

In DMH both shRNAs strongly attenuated SIS-induced aggression, but had no significant effect on freezing (Fig. 6E–G), similar to the effect of Tac2<sup>+</sup> neuron silencing or local infusion of osanetant in this region (Fig. 4E–G and Fig. 5E–G). Conversely, in the dBNSTa shRNA-1 strongly reduced persistent freezing to both the LD and the conditioned tone (Fig. 6C–D, red bars, *post*), but had no effect on acute freezing to the threatening stimuli (Fig. 6C, D, red bars, *during*), or on SIS-induced aggression (Fig. 6B). Notably, unlike the case with Tac2<sup>+</sup> neuron silencing and local osanetant infusion, the stronger shRNA-2 expressed in dBNSTa significantly reduced acute as well as persistent freezing to both the LD and conditioned tone (Fig. 6C–D, I–J, *during*, orange bars). In CeA, Tac2 shRNA2 reduced acute freezing during and after stimulus presentation (Fig. 6I), but had no effect on aggression (Fig. 6H). The fact that local inhibition of Tac2 synthesis or of Tac2<sup>+</sup> neuronal activity yielded similar behavioral effects (Fig. 5K, 6K) supports a requirement for Tac2 release in the effects of SIS.

### Enhancement of Tac2 expression and Tac2<sup>+</sup> neuronal activity mimics the effects of SIS

The foregoing findings indicate that Tac2 is required for the collective behavioral effects of SIS. However, because there is baseline Tac2 expression in these regions in GH mice (Fig. 2B, E), these data do not distinguish whether Tac2 up-regulation *per se* mediates the effects of SIS, or whether Tac2 is simply permissive. Therefore, we asked whether increasing the level and/or release of Tac2 was sufficient to mimic any of the behavioral effects of SIS, in group housed animals.

To do this, we injected intravenously into GH Tac2-IRES-Cre (gene-conserving) driver mice (Fig. S7) Cre-dependent vectors encoding the DREADD neuronal activator hM3D; a Tac2 cDNA or control mCherry using the AAV serotype PHP.B, which crosses the blood-brain barrier (Deverman *et al.*, 2016). Following three weeks to allow for viral expression, all mice (including mCherry-expressing controls) were given CNO in their drinking water for 2

weeks. Mice were then behaviorally tested 20 min following an i.p. CNO injection (Fig. 7A). This procedure was designed to achieve brain-wide Tac2 over-expression and/or neuronal activation in Tac2<sup>+</sup> cells, during both a two-week mock SIS period, as well as during behavioral testing.

Remarkably, combined over-expression of Tac2 and chemogenetic activation of Tac2<sup>+</sup> neurons recapitulated key behavioral effects of SIS in GH mice, including increased aggression and persistent freezing to threats (Fig. 7B–D; summarized in Fig. 7F). In contrast, increasing Tac2 expression, or activating Tac2<sup>+</sup> neurons, on its own was insufficient to yield SIS-like effects in any of our assays (Figs. 7B–E, lavender and cyan bars), as was injection of mCherry-only virus. Histological analysis confirmed expression of mCherry-tagged AAV cargo genes in the dBNSTa, CeA and DMH (Fig. S7A–C), as well as in several additional regions (Fig. S7D–E). The absence of any effects in CNO-treated mCherry virus-injected mice rules out off-target effects of the drug (Gomez *et al.*, 2017).

## DISCUSSION

### Identification of Tac2/NkB as a key mediator of brain responses to chronic SIS

A large number of neuropeptides have been implicated in stress responses, most prominently CRH (reviewed in (Kormos and Gaszner, 2013; Kash *et al.*, 2015; Chen, 2016)). Prior work on the tachykinins in stress has focused primarily on Tac1/Substance P/NkA (Bilkei-Gorzo *et al.*, 2002; Beaujouan *et al.*, 2004; Ebner *et al.*, 2004; Ebner *et al.*, 2008). Previous pharmacological and genetic studies have yielded conflicting results regarding the direction of NkB influences on stress responses (Ebner *et al.*, 2009). Motivated by our previous results in *Drosophila* (Asahina *et al.*, 2014), we identified Tac2/NkB as an important and previously unrecognized mediator of chronic SIS influences on the brain. The finding that tachykinins play a role in the control of social isolation-induced aggression in both flies and mice is consistent with evidence supporting an evolutionary conservation of neuropeptide function in behavior across phylogeny (reviewed in (Bargmann, 2012; Katz and Lillvis, 2014)). It is conceivable that Tac2/NkB may play a role in the well-known effect of solitary confinement to increase violence in humans (Arrigo and Bullock, 2008).

CRH is considered the prototypic stress peptide (Chen, 2016). Approximately 50% of Tac2<sup>+</sup> cells in dBNSTa and CeA co-express CRH (Fig. S7F), raising the possibility that co-release of CRH may play some role in effects of SIS exerted via these structures. However, Tac2 shRNAi and osanetant injections yielded similar effects as Tac2<sup>+</sup> neuronal silencing, while activation of Tac2<sup>+</sup> neurons had no effect unless a Tac2 cDNA was co-expressed. Therefore co-release of CRH is unlikely to explain the results of our chemogenetic manipulations of Tac2<sup>+</sup> neuronal activity. Nevertheless, we cannot exclude that CRH may act genetically upstream or downstream of Tac2 in these structures, to mediate the influences of SIS. Interestingly, there was virtually no expression of CRH among Tac2<sup>+</sup> neurons in DMH, where NkB controls aggression (Fig. S7F).

Our SIS paradigm differs from acute and repeated intermittent stressors (e.g., footshock, restraint, forced swim) not only in its quality, but also in its extended duration and continuous nature. The engagement of the Tac2/NkB system in chronic SIS, therefore, could

reflect any of these differences. However, the fact that systemic delivery of osanetant blocked acute footshock-induced persistent freezing in the LD assay suggests a more general role for the peptide in responses to stressors. A role for Tac2/NkB in consolidation of a conditioned fear memory in CeA has been reported (Andero *et al.*, 2014), but this effect was interpreted to reflect a role in memory consolidation, rather than in stress. Understanding the role of Tac2 in other forms of chronic and acute stress will be an interesting topic for future studies.

### **Tac2/NkB acts in a distributed manner to control multiple components of the SIS response**

With few exceptions (Regev *et al.*, 2011; Regev *et al.*, 2012), most previous studies of neuropeptides in stress have focused on a single brain region, stressor and/or behavior (e.g., the BNST and anxiety assays; reviewed in Kash *et al.*, 2015), and have used a single type of functional perturbation (but see (McCall *et al.*, 2015)). This, together with the variations in stress and behavioral paradigms used in different laboratories, makes it difficult to synthesize studies of the same peptide in different regions to understand how a peptide acts more globally in the brain (Kormos and Gaszner, 2013; Chen, 2016). The multiplexed approach used here permitted comparison of the same perturbation in different brain regions, and of different perturbations in the same brain region, using a battery of behavioral assays. This approach revealed a distributed mode of action in which up-regulation of Tac2 by stress regulated different behavioral effects of SIS in different areas. Such a distributed mechanism is reminiscent of that played by Pigment-Dispersing Factor (PDF) in controlling circadian circuits in *Drosophila* (Taghert and Nitabach, 2012; Dubowy and Sehgal, 2017), or roaming vs. dwelling states in *C. elegans* (Flavell *et al.*, 2013), and may also explain some of the diverse functions of CRH (Regev *et al.*, 2011; Flandreau *et al.*, 2012; McCall *et al.*, 2015).

The fact that local inhibition of Tac2/NkB synthesis, Tac2<sup>+</sup> neuronal activity and NkB receptors yielded qualitatively similar results in each brain region is suggestive of local actions of Tac2. In other systems, NkB acts in an autocrine or paracrine manner on Nk3R-expressing neurons to increase their activity (Navarro, 2013); whether this occurs in the regions studied here is not yet clear. Importantly, our results do not rule out requirements for NkB signaling at distal targets of Tac2<sup>+</sup> neurons as well. The biochemistry of Nk3R action suggests that Tac2/NkB should increase intracellular free calcium via an IP3/DAG pathway (Ebner *et al.*, 2009). In this way, NkB could potentiate the activation of target neurons by glutamate or other excitatory transmitters, and/or promote release of additional peptides.

### **Activation and peptide overexpression in Tac2<sup>+</sup> neurons mimics the effects of SIS**

Injection of stress peptides or receptor agonists can elicit behavioral responses (reviewed in (Koob, 1999; Bruchas *et al.*, 2010; Kormos and Gaszner, 2013)). However, in most studies, injection or transgenic overexpression of a stress peptide does not fully mimic the behavioral effects of stressors. For example, even CRH when exogenously administered to unstressed animals in low arousal conditions does not produce stress-like responses (Koob, 1999).

Using a novel experimental design, we found that overexpression of Tac2 combined with neuronal activation in Tac2<sup>+</sup> cells, but neither manipulation on its own, sufficed to mimic several of the behavioral effects of SIS, in GH mice. This suggests that neuronal activity

may be limiting for observing behavioral effects of neuropeptide overexpression in other systems. This may explain why overexpression of CRH using genetic methods produced different responses, depending on the mode and site of expression (Regev *et al.*, 2011; Flandreau *et al.*, 2012; Regev *et al.*, 2012; Sink *et al.*, 2012; Kash *et al.*, 2015).

Our experiments were enabled by a strategy that allows independent manipulation of Tac2 expression and Tac2<sup>+</sup> neuronal activity, in a brain-wide, noninvasive manner in adult mice (Deverman *et al.*, 2016; Chan *et al.*, 2017), without the need to employ complex transgenic strategies (Lu *et al.*, 2008). More spatially and temporally resolved applications of this approach should reveal precisely where and when enhancing NkB signaling exerts its effects. We anticipate that this approach will prove useful for studying other neuropeptides as well.

### **Increased Tac2/NkB signaling converts stimulus-locked to persistent threat responses**

It was striking to observe that acute freezing responses to threats in GH animals could be converted to persistent ones, simply by artificially increasing Tac2 expression and release. Preliminary data indicate that Tac2 is required for acute freezing in GH animals as well. Together, these data suggest that the up-regulation of Tac2 expression caused by SIS may serve to convert defensive reactions to threats from transient to more enduring responses (Fig. 7H, lower). In this way, the scalable property of neuropeptides – their concentration can vary continuously – may be used to promote persistence, a key component of emotion and related internal states (Anderson and Adolphs, 2014).

With one exception (see below), manipulations of NkB signaling in dBNSTa reduced persistent but not acute (during stimulus) freezing, while manipulations of CeA reduced freezing during as well as following threat stimulus presentation. This dissociation appears consistent with the prevailing view that CeA controls phasic, stimulus-locked defensive responses to threats (“fear”), while dBNSTa controls more persistent responses (“anxiety”) (Walker *et al.*, 2009; Kash *et al.*, 2015). However, in dBNSTa the more potent Tac2 shRNA-2 inhibited acute as well as persistent freezing, while the less potent shRNA-1 only reduced post-stimulus freezing. These data suggest that the effects of Tac2/NkB signaling on acute vs. enduring responses to threats are not determined simply by the region(s) in which the neuropeptide acts, but also by the level of peptide expression and by potentially different thresholds for neuropeptide effects in each area (Fig. 7H). However we cannot exclude the possibility that reciprocal connections between CeA and dBNST (Dong *et al.*, 2001; Dong and Swanson, 2006b, a) may also contribute to the partially overlapping shRNAi phenotypes we observed (Fig. 7G).

### **Nk3R antagonists as potential treatments for isolation-related stress**

Social isolation is well known to promote poor health, clinical psychiatric symptoms and increased mortality in humans (Cacioppo and Hawkley, 2009; Umberson and Montez, 2010; Cacioppo *et al.*, 2015; Holt-Lunstad *et al.*, 2015). Osanetant and several other Nk3R antagonists have been tested in clinical trials as therapies for schizophrenia, bipolar and panic disorder (Spooren *et al.*, 2005). These drugs were well tolerated but abandoned for lack of efficacy (Griebel and Holsboer, 2012). The profound effect of osanetant to prevent

and reverse an SIS-induced deleterious brain state suggests that Nk3R antagonists may merit re-examination as potential treatments for mood disorders caused by extended periods of social isolation (or other stressors) in humans, and in domesticated animals as well.

## STAR METHODS

### KEY RESOURCES TABLE

REAGENT or RESOURCE	SOURCE	IDENTIFIER
Antibodies		
Rabbit polyclonal anti-proNKB	Invitrogen	PA1-16745
Rabbit polyclonal anti-NeuN	Millipore	ABN78
Chicken polyclonal anti-PLP	Millipore	AB15454
Rabbit polyclonal anti-NFIA	Deneen B., Baylor	N/A
Goat anti-rabbit, Alexa Fluor 594	Invitrogen	R37117
Goat anti-chicken, Alexa Fluor 594	Invitrogen	A-11042
Bacterial and Virus Strains		
AAV2-EF1a-DIO-hM4D(Gi)-mCherry	UNC Vector Core	N/A
AAV2-EF1a-DIO-mCherry	UNC Vector Core	N/A
AAV1-CAG-FLEX-eGFP	UNC Vector Core	N/A
AAV5.H1.Tac2-shRNA1.CMV.ZsGreen.SV40	This paper	N/A
AAV5.H1.Tac2-shRNA2.CMV.ZsGreen.SV40	This paper	N/A
AAV5.H1.shRLuc.CMV.ZsGreen.SV40	This paper	N/A
AAVPHP.b-hSyn-Tac2-P2A-mCherry	This paper	N/A
AAVPHP.b-hSyn-Tac2-P2A-GFP	This paper	N/A
AAVPHP.b-hSyn-DIO-hM3D(Gq)-mCherry	This paper	N/A
AAVPHP.b-hSyn-DIO-mCherry	This paper	N/A
Chemicals, Peptides, and Recombinant Proteins		
DAPI	Sigma	D9542
Vectashield	Vector Labs	H-1000
Fluoro-Gel with Tris Buffer	Electron Microscopy Sciences	17985-10
Clozapine N-oxide	Enzo	NS105-0005
Osanetant	Axon	1533; SR 142801
Senktide	Tocris	1068
Digoxigenin-labeled Tac2 RNA probe	This paper	N/A
Digoxigenin-labeled Cfos RNA probe	This paper	N/A
Digoxigenin-labeled CRH RNA probe	This paper	N/A
DNP-labeled Tac2 RNA probe	This paper	N/A
DIG RNA Labeling Mix	Roche	11277073910
DNP-11-UTP	PerkinElmer	NEL555
T7 RNA Polymerase	Roche	10881767001
Anti-digoxigenin-POD	Roche	11207733910

REAGENT or RESOURCE	SOURCE	IDENTIFIER
Anti-DNP antibody, HRP conjugate	PerkinElmer	FP1129
Anti-DNP antibody, Alexa Fluor 488 conjugate	Invitrogen	A11097
Sheep serum	Sigma	S3772
TSA Blocking Reagent	PerkinElmer	FP1020
TSA Plus Biotin Kit	PerkinElmer	NEL749A001KT
TSA Plus DNP (HRP) kit	PerkinElmer	NEL747B001KT
Avidin/biotin blocking kit	Vector Labs	SP-2001
TSA Plus DNP (HRP) System	PerkinElmer	NEL747A001KT
Avidin/Biotin Blocking Kit	Vector Labs	SP-20001
Streptavidin Alexa Fluor 488 conjugate	Invitrogen	S11223
Streptavidin Alexa Fluor 594	Jackson ImmunoResearch	016-580-084
Proteinase K	NEB	P8107S
Yeast tRNA	Sigma	R8759
Calf Thymus DNA	Invitrogen	15633019
Dextran sulfate	Sigma	D8906
Denhardt's Solution 50x	Sigma	D2532
PrimeSTAR Max DNA Polymerase	Takara	R045A
GeneArt Seamless Cloning and Assembly Kit	Invitrogen	A13288
RNAlater	Qiagen	76106
RNAeasy Plus Mini Kit	Qiagen	74134
TURBO DNase	Thermo Fisher	AM2238
Murine RNase Inhibitor	NEB	M0314L
Dynabeads MyOne Silane	Thermo Fisher	37002D
LightCycler 480 SYBR Green	Roche	4887352001
Superscript III Reverse Transcriptase	Life Technologies	18080093
Tac1 Primer	Integrated DNA Technologies	<a href="http://www.idtdna.com">www.idtdna.com</a>
Tac2 Primer	Integrated DNA Technologies	<a href="http://www.idtdna.com">www.idtdna.com</a>
GAPDH Primer	Integrated DNA Technologies	<a href="http://www.idtdna.com">www.idtdna.com</a>
18s Primer	Integrated DNA Technologies	<a href="http://www.idtdna.com">www.idtdna.com</a>
Experimental Models: Organisms/Strains		
C57BL/6N	Charles River	N/A
Balb/c	Charles River	N/A
Tac2-Cre	Harris et al., 2014	N/A
Tac1-Cre	Harris et al., 2014	N/A
Ai6-zsGreen reporter	Madisen et al., 2010	N/A
Ai14-tdTomato reporter	Madisen et al., 2010	N/A
Recombinant DNA		
pAAV.H1.Tac2-shRNA1.CMV.ZsGreen.SV40	This paper	N/A
pAAV.H1.Tac2-shRNA2.CMV.ZsGreen.SV40	This paper	N/A

REAGENT or RESOURCE	SOURCE	IDENTIFIER
pAAV.H1.shRLuc.CMV.ZsGreen.SV40	U Penn Vector Core	PL-C-PV1781
pAAV-GFP	Cell Biolabs Inc	AAV-400
pAAV-hSyn-Tac2-P2A-mCherry	This paper	N/A
pAAV-hSyn-Tac2-P2A-GFP	This paper	N/A
pAAV-hSyn-DIO-hM3D(Gq)-mCherry	Addgene	44361
pAAV-hSyn-DIO-mCherry	Addgene	50459
Software and Algorithms		
Image J	NIH	<a href="https://imagej.nih.gov/ij">https://imagej.nih.gov/ij</a>
Prism 6	GraphPad Software	<a href="http://www.graphpad.com">www.graphpad.com</a>
MATLAB	MathWorks	<a href="http://www.mathworks.com">www.mathworks.com</a>
EthoVision XT	Noldus	<a href="http://www.noldus.com">www.noldus.com</a>
Looming Code, MATLAB	Meister M., Caltech	N/A
Behavior Annotator, MATLAB	Perona P., Caltech	N/A
Behavioral Analysis Code, MATLAB	This paper	N/A
Metamorph	Technical Instrument	<a href="http://www.techinst.com">www.techinst.com</a>
SiDirect 2.0	SiDirect 2.0	<a href="http://sidirect2.mnai.jp/">http://sidirect2.mnai.jp/</a>
Other		
Cannulae (guide, dummy, internal)	Plastics One	N/A
Microinfusion Pump	Harvard Apparatus	<a href="http://www.harvardapparatus.com">www.harvardapparatus.com</a>

## CONTACT FOR REAGENT AND RESOURCE SHARING

Further information and requests for reagents may be directed and will be fulfilled by the Lead Contact David J. Anderson ([wuwei@caltech.edu](mailto:wuwei@caltech.edu)).

## EXPERIMENTAL MODEL AND SUBJECT DEATILS

**Animals**—Wildtype (WT) C57BL/6N male mice (experimental), C57BL/6N female mice (for sexual experience), and BALB/c male mice (intruders) were obtained from Charles River (at 6–10 weeks of age). For visualization of Tac2 and Tac1 expression, we used previously described Cre-dependent Ai6-zsGreen and Ai14-tdTomato fluorescent reporter mice (Madisen et al., 2010), Tac2-IRES2-Cre (Cai et al., 2014), and Tac1-IRES2-Cre knockin mice (obtained from the Allen Institute for Brain Science), which were backcrossed to the C57BL/6N background in the Caltech animal facility. Tac2-IRES-Cre mice were used for Cre-dependent LOF/GOF experiments (Figs. 5, 7). Animals were housed and maintained on a reverse 12-hr light-dark cycle with food and water *ad libitum*. Behavior was tested during the dark cycle. Care and experimental manipulation of animals were in accordance with the National Institute of Health Guide for Care and Use of Laboratory Animals and approved by the Caltech Institutional Animal Care and Use Committee.

## Social isolation stress

WT males (Charles River) were housed in isolation (1 animal per cage), or in groups of 3. Tac2-IRES-Cre males (bred in-house) were housed in isolation, or in groups of 2–5.

Animals were isolated post-weaning, at 8–16 weeks of age. All cage conditions remained otherwise identical for group housed mice compared to isolated animals, and mice were housed on the same rack in the same vivarium. Except where otherwise indicated, social isolation was maintained for at least 2 weeks (this period was extended in the case of surgical experiments, i.e. when adequate time for recovery and viral expression levels were required). All mice were between 12–20 weeks of age at the time of behavioral testing.

## METHOD DETAILS

**Viral constructs**—The AAV2-EF1a-DIO-hM4D(Gq)-mCherry and AAV2-EF1a-DIO-mCherry were acquired from the University of North Carolina (UNC) viral vector core. The pAAV-Tac2-shRNA1-CMV-zsGreen, pAAV-Tac2-shRNA2-CMV-zsGreen, and pAAV-shRLuc-CMV-zsGreen plasmids were constructed (see construction below) and serotyped with AAV5 coat proteins and packaged in-house (see viral packaging below). The pAAV-hSyn-Tac2-P2A-mCherry and pAAV-hSyn-Tac2-P2A-GFP plasmids were constructed (see below) and packaged into AAV-PHP.B (see PHP.B section below). The pAAV-hSyn-DIO-hM3D(Gq)-mCherry and pAAV-hSyn-DIO-mCherry were acquired from Addgene and packaged into AAV-PHP.B (see below).

**Construction of small hairpin RNA expressing AAV vector**—Small hairpin RNA (shRNA) for mouse Tac2 gene (NM\_009312.2) were designed using online designing tool siDirect 2.0 (<http://sidirect2.rnai.jp/>) (Naito et al., 2009).

Oligonucleotides encoding Tac2 shRNAs were purchased from IDT. Oligonucleotides used were as follows: shRNA1, 5'-  
CCGACGTGGTTGAAGAGAACACCGCTTCCTGTCACGGTGTTCTCTTCAACCACGT  
C TTTTTT -3' and 5'-  
AAAAAAGACGTGGTTGAAGAGAACACCGTGACAGGAAGCGGTGTTCTCTTCAAC  
C ACGTCGG -3'; shRNA2, 5'-  
CCGCCTCAACCCCATAGCAATTAGCTTCCTGTCACTAATTGCTATGGGGTTGAGGC  
TTTTTT -3' and 5'-  
AAAAAAGCCTCAACCCCATAGCAATTAGTGACAGGAAGCTAATTGCTATGGGGTT  
G AGGCGG -3' pAAV.H1.shRLuc.CMV.ZsGreen.SV40 (Luc shRNA) plasmid (PL-C-  
PV1781, Penn Vector Core) was used as shRNA AAV vector backbone and control shRNA  
construct.

Entire Luc shRNA plasmid except luciferase shRNA sequence was amplified by PCR with the following primers: shRNA1, Forward -  
AACCACGTCTTTTTTAATTCTAGTTATTAATAGTAATCAA; Reverse -  
CTTCAACCACGTGGCTGGGAAAGAGTGGTCTC; shRNA2, Forward -  
GGTTGAGGCTTTTTTAATTCTAGTTATTAATAGTAATCAA ; Reverse -  
ATGGGGTTGAGGCGGCTGGGAAAGAGTGGTCTC. All PCR reactions were performed using PrimeSTAR Max DNA Polymerase (Takara Bio, Kusatsu, Japan). After PCR amplification, template plasmid was digested by DpnI (NEB, Ipswich, MA) and PCR amplicons were ligated with annealed shRNA oligoes using GeneArt Seamless Cloning and

Assembly Kit (Thermo Fisher Scientific, Waltham, MA) following the manufacturer's instruction.

**Construction of Tac2-overexpression AAV vectors**—Tac2-P2A-mCherry gene fragment was synthesized in the form of IDT gBlocks (see below\*). pAAV-hSyn-Tac2-P2A-mCherry was generated via ligation to AccI/NheI site of pAAV-hSyn-DIO-hM3D(Gq)-mCherry plasmid (Addgene #44361) using DNA Ligation Kit Mighty Mix (Takara Bio, Kusatsu, Japan). To generate pAAV-hSyn-Tac2-P2A-GFP plasmid, entire pAAV-hSyn-Tac2-P2A-mCherry plasmid except mCherry sequence was amplified by PCR with the following primers: Forward - CTCCTCGCCCTTGCTCAC; Reverse - GGC GCGCCATAACTTCGTATAATG and GFP sequence was amplified from pAAV-GFP plasmid (AAV-400, Cell Biolabs Inc, San Diego, CA) with the following primers: Forward - CCTGGACCTATGGTGAGCAAGGGCGAGGAGCTGTTACCGGGGTGGTG; Reverse - AGCATAATTATACGAAGTTATGGCGCGCCCTACTTGAGCTCGAGATCTGAGTAC. Both PCR amplicons were treated with DpnI (NEB) and ligated together using GeneArt Seamless Cloning and Assembly Kit (Thermo Fisher scientific) following the manufacture's instruction.

\*Synthesized Tac2-P2A-mCherry gene fragment:

```
GCTAGCGCCACCATGAGGAGCGCCATGCTGTTTGCGGCTGTCCTCGCCCTCAGCT
TGGCTTGGACCTTCGGGGCTGTGTGTGAGGAGCCACAGGGCAGGGAGGGAGG
CTCAGTAAGGACTCTGATCTCTATCAGCTGCCTCCGTCCCTGCTTCGGAGACTCTA
CGACAGCCGCCCTGTCTCTCTGGAAGGATTGCTGAAAGTGCTGAGCAAGGCTTG
C
GTGGGACCAAAGGAGACATCACTTCCACAGAAACGTGACATGCACGACTTCTTTG
T
GGGACTTATGGGCAAGAGGAACAGCCAACCAGACACTCCCACCGACGTGGTTGA
A
GAGAACACCCCCAGCTTTGGCATCCTCAAAGGAAGCGGAGCTACTAACTTCAGCC
TGCTGAAGCAGGCTGGAGACGTGGAGGAGAACCCTGGACCTATGGTGAGCAAGG
GCGAGGAGGATAACATGGCCATCATCAAGGAGTTCATGCGCTTCAAGGTGCACAT
GGAGGGCTCCGTGAACGGCCACGAGTTCGAGATCGAGGGCGAGGGCGAGGGCC
GCCCCCTACGAGGGCACCCAGACCGCCAAGCTGAAGGTGACCAAGGGTGGCCCCC
TGCCCTTCGCCTGGGACATCCTGTCCCCTCAGTTCATGTACGGCTCCAAGGCCTA
CGTGAAGCACCCCGCCGACATCCCCGACTACTTGAAGCTGTCCTTCCCCGAGGGC
TTCAAGTGGGAGCGCGTGATGAACTTCGAGGACGCGGCGTGGTGACCGTGACC
CAGGACTCCTCCCTGCAGGACGGCGAGTTCATCTACAAGGTGAAGCTGCGCGGC
ACCAACTTCCCCTCCGACGGCCCCGTAATGCAGAAGAAGACCATGGGCTGGGAG
GCCTCCTCCGAGCGGATGTACCCCGAGGACGGCGCCCTGAAGGGCGAGATCAAG
CAGAGGCTGAAGCTGAAGGACGGCGGCCACTACGACGCTGAGGTCAAGACCACC
TACAAGGCCAAGAAGCCCGTGCAGCTGCCCGGCGCCTACAACGTCAACATCAAG
T
TGGACATCACCTCCCACAACGAGGACTACACCATCGTGGAACAGTACGAACGCGC
CGAGGGCCCGCCACTCCACCGGCGGCATGGACGAGCTGTACAAGTAAGGCGCGCC
ATAACTTCGTATAATGTATGCTATACGAAGTTATTAAGAGGTTTCATATTGCTAATAG
```

CAGCTACAATCCAGCTACCATTCTGCATAACTTCGTATAAAGTATCCTATACGAAGT  
TATTCCGGAGTCGAC

**Viral packaging**—rAAVs were produced by polyethylenimine (PEI) triple transfection of HEK293T cells. Briefly, 40 $\mu$ g of equi-molar pHelper, pXR5 and pAAV-trans DNA plasmids were mixed with 120 $\mu$ l of 1mg/ml Polyethylenimine HCl MAX (Polysciences) in PBS and incubated at RT for 5 minutes. 90% confluent HEK293 cells grown on 15cm tissue culture plates were transfected with the plasmid/PEI mixture. Cells were collected 72 hours post transfection, freeze-thawed 3 times and incubated with Benzonase (Millipore) at 5 units/mL for 1 hour. The solution was then centrifuged at 5000xg for 20 minutes. The supernatant was layered on top of a discontinuous gradient of iodixanol and centrifuged at 200,000xg for 2 hours at 18°C. The 40% iodixanol fraction was collected, concentrated, and buffer exchanged with PBS using a Millipore 100kD centrifugal filter. AAV genomic titers were determined by real-time PCR using primers against the ITR and normalized by dilution with PBS to 1 $\times$ 10<sup>12</sup> genome copies per mL virus.

**AAV-PHP.B production and intravenous administration**—The AAV-hSyn-DIO-Tac2-P2A-mCherry, AAV-hSyn-DIO-Tac2-P2A-GFP, AAV-hSyn-DIO-hM3D-mCherry, and AAV-hSyn-DIO-mCherry recombinant AAV genomes were separately packaged into the AAV-PHP.B capsid by triple transfection of HEK293T cells and purified with iodixanol step gradients as previously described (Deverman et al., 2016). 5 $\times$ 10<sup>11</sup> vector genomes (vg) of each virus was administered intravenously (via the retro-orbital sinus) to Tac2-Cre animals individually, or in combination. To equalize the amount of virus given to each mouse, 5 $\times$ 10<sup>11</sup> vg of AAV-PHP.B-hSyn-DIO-mCherry was administered to each animal to bring them up to the amount injected in the double Tac2+hM3DREAAD group. Each animal received a total vector dose of 1 $\times$ 10<sup>12</sup> vg.

**Surgery and cannula implants**—Mice 8–16 weeks old were anesthetized with isoflurane and mounted in a stereotaxic apparatus (Kopf Instruments). Anesthesia was maintained throughout surgery at 1–1.5% isoflurane. The skull was exposed and small burr holes produced dorsal to each injection site using a stereotaxic mounted drill. Virus was backfilled into pulled fine glass capillaries (~50 $\mu$ m diameter at tip) and pressure injections of 300nl were made bilaterally into either the dBNSTa (AP +0.25, ML  $\pm$ 0.85, DV -4.1), DMH (AP -1.3, ML  $\pm$ 0.35, DV -5.6), or CeA (AP -1.4, ML  $\pm$ 2.6, DV -4.73) at a rate of 30nl per minute using a nanoliter injector (Nanoliter 2000, World Precision Instruments) controlled by an ultra microsyringe pump (Micro4, World Precision Instruments). Capillaries remained in place for 5 minutes following injections to allow for full diffusion of virus and to reduce backflow up the injection tract. Skin above the skull was then drawn together and sealed with GLUture (Zoetis). For bilateral cannula implantations, single or double guide cannula (custom, Plastics One) aimed 0.5mm above each region were implanted and held in place with dental cement (Parkell). Compatible dummy cannulas with a 0.5mm protrusion at the tip were inserted to prevent cannula clogging. Directly following surgery, mice were given a subcutaneous injection of ketoprofen (2mg/kg) and supplied with drinking water containing 400mg/L sulphamethoxazole and 200mg/L ibuprofen and monitored for 7 days. Dummies

were replaced every 2–3 days to keep cannula tracts clean. All injections were subsequently verified histologically.

**Immunohistochemistry**—Immunofluorescence staining proceeded as previously described (Anthony et al., 2014; Cai et al., 2014; Hong et al., 2014; Kunwar et al., 2015). Briefly, mice were perfused transcardially with 0.9% saline followed by 4% paraformaldehyde (PFA) in 1XPBS. Brains were extracted and post-fixed in 4% PFA overnight at 4°C followed by 48 hours in 15% sucrose. Brains were embedded in OCT mounting medium, frozen on dry ice, and stored at –80°C for subsequent sectioning. Sections 40–50 µm thick were cut on a cryostat (Leica Biosystems). Sections were either directly mounted onto Superfrost slides for histological verification of injections/cannula placements or were cut free floating for antibody staining. For antibody staining, brain sections were washed 3× in 1XPBS and blocked in PBS-T (0.3% Triton X-100 in 1XPBS) with 10% normal goat or donkey serum for 1hr at room temperature (RT). Sections were then incubated in primary antibody diluted in blocking solution at 4°C for 48–72 hours. We stained for neurokinin B (rabbit anti-proNKB; 1:1000; Invitrogen); the glial marker nuclear factor I-A (rabbit anti-mouse NFIA; 1:1000; Deneen lab) (Deneen et al., 2006); the oligodendrocyte marker proteolipid protein (chicken anti-PLP; 1:1,000; Millipore) or the nuclear marker NeuN (rabbit anti-NeuN; 1:1000; Millipore). Sections were then washed 3× and incubated in secondary antibodies diluted in blocking buffer (goat anti-rabbit, goat anti-chicken, Alexa Fluor 594, 1:500) overnight at 4°C. Sections were then washed 3X, incubated for 20 minutes at RT in DAPI diluted in 1XPBS (1:2000) for counterstaining, washed again, mounted on Superfrost slides, and coverslipped for imaging on a confocal microscope (Olympus FluoView FV1000).

**Fluorescent in situ hybridization**—Digoxigenin (DIG)-labeled *Tac2*, *Cfos*, *Crh* RNA probes and dinitrophenyl (DNP)-labeled *Tac2* probe were generated following a previously described protocol (<http://help.brain-map.org/display/mousebrain/Documentation>) (Lein et al., 2007) with the following primer sets: *Tac2*; Forward - AGCCAGCTCCCTGATCCT; Reverse -TTGCTATGGGGTTGAGGC (NM\_009312.2, 36–608bp) *Cfos*; Forward - agaatccgaagggaacgg and Reverse -ggagccagatgtggatg (NM\_010234.2, 560–1464bp) *Crh*; Forward - agggaggagaagagagc and Reverse agccaccctcaagaatg (NM\_205769.3, 219–1185bp). Fluorescent in situ hybridization (FISH) or double fluorescent in situ hybridization (dFISH) was carried out according to the protocol used in (Thompson et al., 2008) with modifications. Briefly, mice were transcardially perfused with 1 × PBS followed by 4% paraformaldehyde/PBS (PFA) in 1 × PBS. Brains were fixed in 4% PFA 3–4 hours at 4°C and cryoprotected for overnight in 15% sucrose at 4°C. Brains were embedded in OCT Compound (Fisher Scientific) and cryosectioned in 30 µm thickness and mounted on Superfrost Plus slides (Fisher Scientific). Sections were fixed in 4% PFA for 30 min, acetylated with 0.25% acetic anhydride in 0.1 M triethanolamine for 10 min, dehydrated with increasing concentrations of EtOH (50, 70, 95 and 100%), gently treated with proteinase K (6.3 µg/mL in 0.01M Tris-HCl pH7.4 and 0.001M EDTA) for 10 min, and fixed in 4% PFA for 20 min. All procedures were performed at room temperature (RT). The hybridization buffer contained 50% deionized formamide, 3 × standard saline citrate (SSC), 0.12 M PB (pH 7.4), 10% dextran sulfate, 0.12 mg/ml yeast tRNA, 0.1 mg/mL calf thymus

DNA, and 1× Dehardt solution. The sections were prehybridized at 63°C in hybridization buffer for 30 min and then hybridized with RNA probes (300 ng/ml for each probe) in hybridization buffer at 63 °C for 16 hours. After hybridization, the sections were washed with 5 × SSC for 10 min, 4× SSC / 50% formamide for 20 min, 2× SSC / 50% formamide for 30min, and 0.1× SSC for 20min twice each at 61 °C. The sections were blocked with 4% sheep serum in TNT buffer (Tris-HCl pH7.5, 0.15 M NaCl and 0.00075% tween 20) for 30 min and TNB Blocking buffer (TSA blocking reagent, PerkinElmer, Waltham, MA) for 30 min at RT. The sections were incubated with anti-digoxigenin-POD antibody (1:600, Roche Diagnostics) in TNB buffer for overnight at RT. The sections were washed with TNT buffer and tyramide-biotin signal amplification was performed using the TSA Plus Biotin Kit (PerkinElmer) and signals were visualized after 1 hr incubation with Alexa Fluor 594 Streptavidin (Jackson ImmunoResearch) or Alexa Fluor 488 Streptavidin (Invitrogen) at RT. The sections were washed with TNT buffer and fixed with 4% PFA for 20 min at RT, washed with PBS, blocked with avidin/biotin blocking kit (Vector), and then treated with 0.3% H<sub>2</sub>O<sub>2</sub> for 15 min at RT. Subsequently, the sections were washed with PBS, blocked with TNB blocking buffer for 20 min at RT, and incubated with anti-DNP HRP conjugated antibody (1:250, PerkinElmer) in TNB blocking buffer for overnight at RT. On the following day, the sections were washed with TNT buffer and tyramide-DNP signal amplification was performed using the TSA Plus DNP (HRP) Kit (PerkinElmer) and signals were visualized with Anti-DNP Alexa Fluor 488 conjugated antibody (1:125, Invitrogen) at RT. The Sections were counterstained with DAPI (0.5ug/mL in PBS), washed with 1 × PBS, and coverslipped using Fluoro-Gel with Tris Buffer (Electron Microscopy Sciences). Tissue images of entire coronal brain sections were taken using a slide-scanner (VS120-S6-W, Olympus) or a confocal microscope (FluoView FV1000, Olympus) and cells positive for the probes were counted as described below.

**Cell counting**—Following confocal or slide-scanner imaging, quantification of labeled cells was performed using ImageJ and Metamorph. Cells were counted by an observer blind to experimental conditions. Brain images were converted to greyscale (16-bit) in ImageJ and adjusted using automatic thresholding and watershed separation. Cells were either counted automatically using ImageJ’s particle analysis algorithm (random sections were counted manually to cross-check that automated scoring was consistent with manual human scoring); otherwise, cells were counted manually using MetaMorph. Cells that were not entirely contained within a given region of interest (ROI) were excluded from analyses. Relative fluorescent intensities (for cell body or projection terminal labeling with a fluorescent protein) were measured automatically using MetaMorph for a given ROI. Raw cell counts within an ROI were divided by the size of the ROI (mm<sup>2</sup>) to produce the number of positively labeled cells/mm<sup>2</sup>.

**Quantitative real-time reverse transcription PCR**—Group housed or isolated (30 minutes, 24 hours, 2 weeks) mice were decapitated and brains were quickly removed and placed in RNA Later (Qiagen) at 4°C. Tissue from dBNSTa, DMH, CeA, ACC, and dHPC was micro-dissected and placed in RNA Later. Tissue was then homogenized and RNA purified using an RNAeasy Plus Mini Kit (Qiagen). 150ng of total RNA/region/condition was then incubated with 3µl of Turbo DNase, 1µl of Murine RNase Inhibitor, in 1× Turbo

DNase buffer for 15 minutes at 37°C to remove any contaminating genomic DNA. Samples were subsequently purified using Dynabeads MyOne Silane beads and eluted in 11 µl. The eluted RNA was used as input into a 20µl reverse transcriptase reaction (SuperScript III). 1µl of 100µM random 9mers (NNNNNNNNN - IDT corporation) served as primers. The reverse transcriptase reaction was inactivated at 70°C prior to qPCR analysis on the LightCycler 480 Instrument II. The following primers, ordered from Integrated DNA Technologies, were used: Tac1 (Forward – GATGAAGGAGCTGTCCAAGC; Reverse – TCACGAAACAGGAAACATGC); Tac2 (Forward– GCCATGCTGTTTGCGGCTG; Reverse – CCTTGCTCAGCACTTTCAGC); GAPDH (Forward – TGAAGCAGGCATCTGAGGG; Reverse – CGAAGGTGGAAGAGTGGGAG); and 18s (Forward – GCAATTATCCCCATGAACG; Reverse – GGGACTTAATCAACGCAAGC). GAPDH and 18s served as housekeeping genes to which Tac1 and Tac2 were normalized. Primers were resuspended in ddH2O to 100µM. A 25µM mix of each primer was used as input for qRT-PCR reaction. Four technical replicates were run for each sample primer pair and the Cp (Crossing Point) value was determined using Lightcycler II Software. The median value of the four technical replicates was used as the representative value for the set. Final mRNA fold increase values were determined by normalizing raw fluorescent values of experimental animals to controls using the following formula:  $2^{-(\text{Cycles Control} - \text{Cycles Experimental})}$ . Thus for example, if the control sample required 8 cycles and the experimental sample 3 cycles to reach the Cp, then the fold-increase for experimental/control would be  $2^{(8-3)} = 2^5 = 32$ -fold.

**Resident intruder assay**—Testing for aggression using the resident intruder assay (Blanchard et al., 2003) proceeded similarly to as previously described (Hong et al., 2015; Hong et al., 2014; Lee et al., 2014). Briefly, experimental mice (“residents”) were transported in their homecage to a novel behavior testing room (cagemates in group housed mice were removed from the homecage prior to transport for this and all other behavioral tests), where they acclimated for 5–15 minutes. Homecages were then slotted into a customized behavioral chamber lit with a surround panel of infrared lights and equipped with two synchronized infrared video cameras (Pointgrey) placed at 90-degree angles from each other to allow for simultaneous behavior recording with a front and top view. Synchronized video was acquired using Hunter 4.0 software (custom, Pietro Perona lab, Caltech). Following a two-minute baseline period, an unfamiliar male BALB/c mouse (“intruder”) was placed in the homecage of the resident for 10 minutes and mice were allowed to freely interact. Group housed BALB/c males were used as intruders because they are a relatively submissive strain, thereby reducing any intruder initiated fighting. Behavior videos were hand annotated by an observer blind to experimental conditions (Behavior Annotator, Piotr’s MATLAB toolbox; <http://vision.ucsd.edu/~pdollar/toolbox/doc/>). Fighting bouts were scored on a frame-by-frame basis and were defined as a frame in which the resident male was currently engaged in an episode of biting or intense aggressive behavior immediately surrounding a biting episode. Annotation files were then batch analyzed for behavior, including number of fighting bouts, using in-house customized programs in MATLAB (A. Kennedy, Caltech).

**Looming disk assay**—Freezing behavior to presentation of an overhead looming disk proceeded as previously described (Kunwar et al., 2015; Yilmaz and Meister, 2013). Briefly, mice were transported to a novel behavioral testing room. After 5 minutes of acclimation, mice were placed inside a novel, custom-built open top Plexiglas arena (48 × 48 × 30 cm) covered with a flat screen monitor placed directly above and illumination provided by infrared LEDs (Marubeni). Mice were given a 5 minute baseline period in the arena, following which entry into the center of the arena triggered presentation of a single, 10 second overhead looming disk stimulus (comprised of a single looming disk presentation 0.5 seconds in duration, which was repeated 10 times with an inter-stimulus interval of 0.5 seconds). The stimulus was controlled by custom MATLAB code (M. Meister, Caltech) run on dedicated computer in an adjacent room. Mice remained in the area for an additional 2 minutes before being transported back. Behavior was recorded using a video recorder attached to a laptop equipped with video capture software (Corel VideoStudio Pro). Acute freezing behavior to the looming disk (“during”), as well as in the 30 seconds following the last disk (“post”) were scored manually (Behavior Annotator, MATLAB) by an observer blind to environmental conditions.

**Tone fear conditioning and shock reactivity**—The protocol for tone trace fear conditioning occurred as previously described (Cushman et al., 2014) in fear conditioning boxes previously described in detail (Haubensak et al., 2010; Kunwar et al., 2015). Briefly, mice were transported in squads of four on a white cart to a novel behavioral testing room containing 4, sound-attenuating fear-conditioning chambers (Med Associates). This “training context” was comprised of flat grid flooring (wired to a shock generator and scrambler for footshock delivery, Med Associates), houselights, and the presence of an internal fan for background noise. Chambers were sprayed with a 70% Simple Green solution on the underlying chamber pan to generate a unique contextual scent and chambers were cleaned with 70% EtOH between squads. Trace fear conditioning consisted of a 3 minute baseline period followed by 3 tone-shock trials consisting of a 20 second tone conditional stimulus (CS; 75dB, 2800 Hz), a 20 second trace interval and a 2 second footshock unconditional stimulus (US; 0.7mA). The inter-trial interval (ITI) between trials was 60 seconds. Mice remained in the chambers an additional 60 seconds before transport back to the vivarium. The following day, mice were transported in fresh cardboard boxes to a novel behavioral testing room consisting of 4 distinct fear-conditioning boxes to test for tone fear. The “test context” consisted of the houselights and fan turned off, uneven grid flooring, a 1% acetic acid scent and a black plastic insert used to generate a triangular roof. Testing occurred identical to training with the exception that shocks were omitted from test trials to allow for behavior assessment to the tone. A single shock was administered in the last minute of testing to assess activity burst responding to the shock. This allowed us to assess reactivity to the shock under our various manipulations performed at test without disrupting fear acquisition by performing manipulations during training. All experimental manipulations and data displayed in the manuscript were performed during the test phase of fear conditioning (training data not shown). Training and testing context were counterbalanced across mice. Freezing behavior during the baseline period as well as during each tone presentation (“during”) and trace interval (“post”) were assessed as previously described (Zelikowsky et al., 2014) using automated near-infrared video tracking equipment

and computer software (VideoFreeze, Med Associates). Shock reactivity (motion, arbitrary units) was measured during the 2 second shock US as well as the 3 seconds immediately following. Acute footshock stress (Fig. S3L-M) was generated by delivering 4 unsignaled administrations of a 2 sec, .7mA footshock following a 3 minute baseline period. The ITI was 90 seconds.

**Ultrasonic sound stimulus assay**—Behavior was tested as previously described (Mongeau et al., 2003). Briefly, mice were brought into a novel experimental testing room in their homecages and allowed to acclimate for 5 minutes. Behavior in the homecage to an ultrasonic sound stimulus (USS) was then recorded using a digital video camera connected to a portable laptop equipped with video capture software (Corel VideoStudio Pro). Mice received a two-minute baseline period behavior followed by three, 1 minute presentations of the USS (100ms frequency sweeps between 17 and 20 kHz, 85 dB, alternately ON 2 sec/OFF 2 sec) with a 1-minute inter-trial interval. Following testing mice were returned to the vivarium. Freezing behavior to each USS and post-USS period (ITI) was manually scored by an observer blind to experimental conditions (Behavior Annotator, MATLAB).

**Open field test**—Open field testing (OFT) occurred as previously described (Anthony et al., 2014; Cai et al., 2014; Kunwar et al., 2015) to examine anxiety-like behavior (thigmotaxis) in a novel open arena. Briefly, mice were brought into a novel behavior testing room in squads of 4. They were then individually placed in plastic open top arenas (50 × 50 × 30cm) and allowed to freely move for a 10 minute period. Video was captured using an overhead mounted video camera connected to a dedicated computer in an adjacent room equipped with Mediacruise (Canopus) video capture software. Ethovision software was used to generate trajectory maps and analyze time spent in the center of the arena (center 50%) and average velocity.

**Elevated plus maze**—Elevated plus maze (EPM) testing occurred as previously described (Cai et al., 2014; Kunwar et al., 2015). Briefly, mice were brought into a behavioral testing room and tested on anxiety-like behavior on an elevated plus maze. The EPM was comprised of a platform (74cm above the floor) with four arms – two opposing open arms (30 × 5cm) and two opposing closed arms (30 × 5 × 14cm). Mice were placed in the center of the EPM and their behavior was tracked for 5 minutes using Mediacruise (Canopus) for video capture and Ethovision for trajectory maps, analyses of time spent in each arm, and number of entries. Mice were also scored for whether or not they jumped off of the center of the platform within 5 seconds of being initially placed on the EPM.

**Acoustic startle response**—Startle responding to an acoustic stimulus (Koch, 1999) was measured using a startle chamber (SR-LAB; San Diego Instruments) as previously described (Shi et al., 2003). Briefly, mice (in squads of 3) were brought into a novel behavioral testing room in their homecages and allowed to acclimate for 5–10 minutes. Mice were then placed into sound-attenuating startle chambers comprised of a Plexiglas cylinder (5.1cm diameter) mounted on a platform (20.4 × 12.7 × 0.4 cm) with a piezoelectric accelerometer unit attached below to detect startle motion. The chambers contained an overhead loudspeaker and light. Following a 3 minute baseline, mice were presented with a

series of 8 noise presentations ramping up from 67–124dB (67, 78, 86, 95, 104, 109, 115, 124dB) across a 4 minute period (~30 sec variable inter-trial interval; ITI). The delivery of acoustic stimuli and acquisition of startle motion was controlled by SR-LAB software on a dedicated computer. Prior to each behavioral testing session, sound levels were calibrated with a sound-level meter (Radio Shack), and response sensitivities were calibrated using the SR-LAB Startle Calibration System. Startle chambers were cleaned with 70% EtOH between squads.

**Flinch-vocalize-jump assay**—Sensitivity to a noxious footshock stimulus was assessed using the flinch-vocalize-jump assay (Kim et al., 1991). Mice were transported to a behavioral testing room and individually tested in a fear conditioning box (Med Associates) for reactivity to a series of manually delivered shocks ramping up in amplitude. Shocks were administered every 5 seconds beginning from 0.05 mA until 0.6 mA, with each shock increasing by 0.05 mA. The shock intensity level at which the mouse displayed flinching (first perceptible reaction to the shock), vocalization (sound audible to a human observer), and jumping (simultaneous lifting of all 4 paws off the grid) was noted for each mouse.

**Social interaction assay**—Mice were tested for interactive behavior towards a novel mouse using the social interaction assay. Behavior proceeded as previously described (Hsiao et al., 2013). Briefly, mice were brought to a behavioral testing room in squads of 4 and individually placed in a long Plexiglass apparatus (50 × 75 cm) consisting of three chambers – a center chamber and two side chambers each containing an empty pencil cup flipped upside-down. Following a 5 minute baseline period, an unfamiliar male mouse (BALB/c) was placed under one pencil cup, and a novel object (50 mL falcon tube cut in half) was placed under the other (placements counterbalanced across mice). Sociability across a 10 minute time period was assessed. Video was captured using an overhead mounted video camera connected to a dedicated computer in an adjacent room equipped with Mediacruise (Canopus) video capture software. Ethovision software (Noldus) was used to analyze time spent in each chamber and generate an output file containing information on XY coordinates (location). XY coordinates were then used to generate heat maps reflecting the amount of time spent at each location in the social interaction apparatus (Matlab).

**Rat exposure assay**—Behavior was tested as previously described in (Kunwar et al., 2015). Briefly, mice were tested for behavior towards an intact rat predator (Blanchard et al., 2005), weighing 300–500 grams. Mice were brought in their homecage into a novel testing environment. Behavior was recorded using a digital video camera attached to a portable laptop running video acquisition software (Corel VideoStudio Pro). Following a 3 minute baseline period, a rat was lowered onto one side of the mouse's homecage in a custom-made mesh enclosure (16 × 11 × 15 cm) for a 5 minute time period. In order to assess where the mouse spent its time, the home cage was divided into three equal zones with Zone 1 being closest to the rat and Zone 3 farthest. Time spent in each zone as well freezing behavior (not shown) was calculated using EthovisionXT software (Noldus).

**Pharmacology**—Mice were administered the Nk3R antagonist osanetant (Axon Medchem, Axon 1533) either systemically or intra-brain region. Osanetant was dissolved in

saline with 0.1% Tween 20 (vehicle). For systemic administration mice received an intraperitoneal (i.p.) injection (5 mg/kg) 20 minutes prior to behavioral testing. For microinfusions, guide cannula were removed from mice and replaced with injector cannula (Plastics One), which protruded 0.5mm from the tip of the guide cannula. Injectors were attached to 5  $\mu$ l Hamilton syringes with PE tubing (Plastics One) and mounted on a microinfusion pump (Harvard Apparatus) for controlled infusion of osanetant (0.3  $\mu$ l vehicle with 375 ng dose per site injected across 6 minutes). In a separate experiment, mice were administered the Nk3R agonist, Senktide (Tocris, 1068). Senktide was dissolved in saline and injected i.p. (2mg/kg) 20 minutes prior to behavioral testing. For experiments using systemic administration of clozapine-N-oxide (CNO), CNO (Enzo Life Sciences-Biomol, BML-NS105-0005) was dissolved in saline (9 g/L NaCl) and injected (i.p.) at 5 mg/kg for hM4DREADD silencing or 2 mg/kg for hM3DREADD activation 20 minutes prior to behavioral testing. CNO was also administered chronically in drinking water (0.5mg CNO/100ml water).

## QUANTIFICATION AND STATISTICAL ANALYSES

All behavioral data was scored by a trained observer blind to experimental conditions, or scored using an automated system (Ethovision, Med Associates). Data were then processed and analyzed using MATLAB, Excel, Prism 6, and G\*Power. Statistical analyses were conducted using ANOVAs followed by Bonferroni post hoc tests, Fisher's LSD tests, and unpaired t tests when appropriate. The n value, the mean values  $\pm$ SEM for each data set, and statistically significant effects are reported in each figure/figure legend. The significance threshold was held at  $\alpha=0.05$ , two-tailed (not significant, ns,  $p>.05$ ; \* $p<0.05$ ; \*\* $p<0.01$ ; \*\*\* $p<0.001$ ). Full statistical analyses corresponding to each data set, including 95% confidence intervals (CIs) and effect size ( $\eta^2$ ), are presented in Table S1.

## Supplementary Material

Refer to Web version on PubMed Central for supplementary material.

## Acknowledgments

We thank X. Da and X. Wang for help with behavior scoring and histology; M. McCardle and Y. Huang for genotyping; J. Costanza for mouse colony management, C. Chiu and G. Mancuso for lab management and administrative assistance; A. Choe for help with behavioral testing, the diagrams in Fig. 2A and fruitful discussion; A. Kennedy for generating MATLAB code for behavioral data processing and the models in Fig. 7H; Z. Turan and M. Meister for help implementing the LD assay; W. Wu for initial help on the acoustic startle assay; P. Kunwar for initial help on the ultrasonic sound stimulus assay; T. Anthony for initial help with RNA isolation and purification, and all the members of the Anderson lab for their support. We thank Ben Deneen for providing the NFIA antibody, Mitchell Guttman and his lab for providing resources and sharing use of qRT-PCR reagents and equipment; the CLOVER institute for generation of PHP.B constructs; and the Perona lab for continued help with customized behavioral tracking and analyses software. This work was supported by grants from the National Institute of Mental Health, Gordon Moore Foundation, Ellison Medical Research Foundation and Simons Foundation to D.J.A. and by a NARSAD Young Investigator Award, the L'OREAL for Women in Science award, and an NIMH K99 Pathway to Independence award to M.Z. D.J.A. is an Investigator of the Howard Hughes Medical Institute.

## References

An D, Chen W, Yu DQ, Wang SW, Yu WZ, Xu H, Wang DM, Zhao D, Sun YP, Wu JC, Tang YY, Yin SM. Effects of social isolation, resocialization and age on cognitive and aggressive behaviors of

- Kunming mice and BALB/c mice. *Animal science journal = Nihon chikusan Gakkaiho*. 2017; 88:798–806. [PubMed: 27619417]
- Andero R, Daniel S, Guo JD, Bruner RC, Seth S, Marvar PJ, Rainnie D, Ressler KJ. Amygdala-Dependent Molecular Mechanisms of the Tac2 Pathway in Fear Learning. *Neuropsychopharmacology : official publication of the American College of Neuropsychopharmacology*. 2016; 41:2714–2722. [PubMed: 27238620]
- Andero R, Dias BG, Ressler KJ. A role for Tac2, NkB, and Nk3 receptor in normal and dysregulated fear memory consolidation. *Neuron*. 2014; 83:444–454. [PubMed: 24976214]
- Anderson DJ. Circuit modules linking internal states and social behaviour in flies and mice. *Nature reviews Neuroscience*. 2016; 17:692–704. [PubMed: 27752072]
- Anderson DJ, Adolphs R. A Framework for Studying Emotions across Species. *Cell*. 2014; 157:187–200. [PubMed: 24679535]
- Anthony TE, Dee N, Bernard A, Lerchner W, Heintz N, Anderson DJ. Control of stress-induced persistent anxiety by an extra-amygdala septohypothalamic circuit. *Cell*. 2014; 156:522–536. [PubMed: 24485458]
- Arrigo BA, Bullock JL. The psychological effects of solitary confinement on prisoners in supermax units: reviewing what we know and recommending what should change. *International journal of offender therapy and comparative criminology*. 2008; 52:622–640. [PubMed: 18025074]
- Asahina K, Watanabe K, Duistermars BJ, Hoopfer E, Gonzalez CR, Eyjolfsdottir EA, Perona P, Anderson DJ. Tachykinin-expressing neurons control male-specific aggressive arousal in *Drosophila*. *Cell*. 2014; 156:221–235. [PubMed: 24439378]
- Bargmann CI. Beyond the connectome: how neuromodulators shape neural circuits. *BioEssays : news and reviews in molecular, cellular and developmental biology*. 2012; 34:458–465.
- Beaujouan JC, Torrens Y, Saffroy M, Kemel ML, Glowinski J. A 25 year adventure in the field of tachykinins. *Peptides*. 2004; 25:339–357. [PubMed: 15134859]
- Berridge KC. Motivation concepts in behavioral neuroscience. *Physiology & Behavior*. 2004; 81:179–209. [PubMed: 15159167]
- Bilkei-Gorzo A, Racz I, Michel K, Zimmer A. Diminished anxiety- and depression-related behaviors in mice with selective deletion of the Tac1 gene. *The Journal of neuroscience : the official journal of the Society for Neuroscience*. 2002; 22:10046–10052. [PubMed: 12427862]
- Blanchard DC, Blanchard RJ, Griebel G. Defensive responses to predator threat in the rat and mouse. *Current protocols in neuroscience*. 2005; Chapter 8(Unit 8):19.
- Blanchard DC, Griebel G, Blanchard RJ. The Mouse Defense Test Battery: pharmacological and behavioral assays for anxiety and panic. *European journal of pharmacology*. 2003; 463:97–116. [PubMed: 12600704]
- Bourin M, Petit-Demoulière B, Nic Dhonnchadha B, Hascöet M. Animal models of anxiety in mice. *Fundamental & Clinical Pharmacology*. 2007; 21:567–574. [PubMed: 18034657]
- Bruchas MR, Land BB, Chavkin C. The dynorphin/kappa opioid system as a modulator of stress-induced and pro-addictive behaviors. *Brain research*. 2010; 1314:44–55. [PubMed: 19716811]
- Cacioppo JT, Cacioppo S, Capitanio JP, Cole SW. The Neuroendocrinology of Social Isolation. *Annu Rev Psychol*. 2015; 66:733–767. [PubMed: 25148851]
- Cacioppo JT, Hawkley LC. Perceived social isolation and cognition. *Trends Cogn Sci*. 2009; 13:447–454. [PubMed: 19726219]
- Cacioppo S, Capitanio JP, Cacioppo JT. Toward a neurology of loneliness. *Psychological bulletin*. 2014; 140:1464–1504. [PubMed: 25222636]
- Cai H, Haubensak W, Anthony TE, Anderson DJ. Central amygdala PKC-delta(+) neurons mediate the influence of multiple anorexigenic signals. *Nature neuroscience*. 2014; 17:1240–1248. [PubMed: 25064852]
- Chan KY, Jang MJ, Yoo BB, Greenbaum A, Ravi N, Wu WL, Sanchez-Guardado L, Lois C, Mazmanian SK, Deverman BE, Gradinaru V. Engineered AAVs for efficient noninvasive gene delivery to the central and peripheral nervous systems. *Nature neuroscience*. 2017; 20:1172–1179. [PubMed: 28671695]
- Chen, A. Genetic Dissection of the Neuroendocrine and Behavioral Responses to Stressful Challenges. In: Pfaff, D., Christen, Y., editors. *Stem Cells in Neuroendocrinology*. Cham (CH): 2016.

- Cho JR, Treweek JB, Robinson JE, Xiao C, Bremner LR, Greenbaum A, Gradinaru V. Dorsal Raphe Dopamine Neurons Modulate Arousal and Promote Wakefulness by Salient Stimuli. *Neuron*. 2017; 94:1205–1219. e1208. [PubMed: 28602690]
- Conklin BR, Hsiao EC, Claeysen S, Dumuis A, Srinivasan S, Forsayeth JR, Guettier JM, Chang WC, Pei Y, McCarthy KD, Nissenson RA, Wess J, Bockart J, Roth BL. Engineering GPCR signaling pathways with RASSLs. *Nature methods*. 2008; 5:673–678. [PubMed: 18668035]
- Culman J, Unger T. Central Tachykinins - Mediators of Defense Reaction and Stress Reactions. *Canadian Journal of Physiology and Pharmacology*. 1995; 73:885–891. [PubMed: 8846426]
- Cushman JD, Moore MD, Olsen RW, Fanselow MS. The role of the delta GABA(A) receptor in ovarian cycle-linked changes in hippocampus-dependent learning and memory. *Neurochemical research*. 2014; 39:1140–1146. [PubMed: 24667980]
- Deneen B, Ho R, Lukaszewicz A, Hochstim CJ, Gronostajski RM, Anderson DJ. The transcription factor NFIA controls the onset of gliogenesis in the developing spinal cord. *Neuron*. 2006; 52:953–968. [PubMed: 17178400]
- Deverman BE, Pravdo PL, Simpson BP, Kumar SR, Chan KY, Banerjee A, Wu WL, Yang B, Huber N, Pasca SP, Gradinaru V. Cre-dependent selection yields AAV variants for widespread gene transfer to the adult brain. *Nature biotechnology*. 2016; 34:204–209.
- Dong HW, Swanson LW. Projections from bed nuclei of the stria terminalis, anteromedial area: Cerebral hemisphere integration of neuroendocrine, autonomic, and behavioral aspects of energy balance. *J Comp Neurol*. 2006a; 494:142–178. [PubMed: 16304685]
- Dong HW, Swanson LW. Projections from bed nuclei of the stria terminalis, dorsomedial nucleus: implications for cerebral hemisphere integration of neuroendocrine, autonomic, and drinking responses. *J Comp Neurol*. 2006b; 494:75–107. [PubMed: 16304681]
- Dong HW, Petrovich GD, Swanson LW. Topography of projections from amygdala to bed nuclei of the stria terminalis. *Brain research Brain research reviews*. 2001; 38:192–246. [PubMed: 11750933]
- Dubowy C, Sehgal A. Circadian Rhythms and Sleep in *Drosophila melanogaster*. *Genetics (Genetics)*. 2017:1373–1397.
- Ebner K, Muigg P, Singewald G, Singewald N. Substance P in stress and anxiety: NK-1 receptor antagonism interacts with key brain areas of the stress circuitry. *Annals of the New York Academy of Sciences*. 2008; 1144:61–73. [PubMed: 19076365]
- Ebner K, Rupniak NM, Saria A, Singewald N. Substance P in the medial amygdala: emotional stress-sensitive release and modulation of anxiety-related behavior in rats. *Proceedings of the National Academy of Sciences of the United States of America*. 2004; 101:4280–4285. [PubMed: 15024126]
- Ebner K, Sartori SB, Singewald N. Tachykinin receptors as therapeutic targets in stress-related disorders. *Curr Pharm Des*. 2009:1647–1674. [PubMed: 19442179]
- Emonds-Alt X, Bichon D, Ducoux JP, Heaulme M, Miloux B, Poncelet M, Proietto V, Van Broeck D, Vilain P, Neliat G, et al. SR 142801, the first potent non-peptide antagonist of the tachykinin NK3 receptor. *Life sciences*. 1995; 56:PL27–32. [PubMed: 7830490]
- Fanselow MS. Conditioned and unconditional components of post-shock freezing. *The Pavlovian journal of biological science*. 1980; 15:177–182. [PubMed: 7208128]
- Flandreau EI, Ressler KJ, Owens MJ, Nemeroff CB. Chronic overexpression of corticotropin-releasing factor from the central amygdala produces HPA axis hyperactivity and behavioral anxiety associated with gene-expression changes in the hippocampus and paraventricular nucleus of the hypothalamus. *Psychoneuroendocrinology*. 2012; 37:27–38. [PubMed: 21616602]
- Flavell SW, Pokala N, Macosko EZ, Albrecht DR, Larsch J, Bargmann CI. Serotonin and the neuropeptide PDF initiate and extend opposing behavioral states in *C. elegans*. *Cell*. 2013; 154:1023–1035. [PubMed: 23972393]
- Gomez JL, Bonaventura J, Lesniak W, Mathews WB, Sysa-Shah P, Rodriguez LA, Ellis RJ, Richie CT, Harvey BK, Dannals RF, Pomper MG, Bonci A, Michaelides M. Chemogenetics revealed: DREADD occupancy and activation via converted clozapine. *Science*. 2017; 357:503–507. [PubMed: 28774929]
- Griebel G, Holsboer F. Neuropeptide receptor ligands as drugs for psychiatric diseases: the end of the beginning? *Nature reviews Drug discovery*. 2012:1–17.

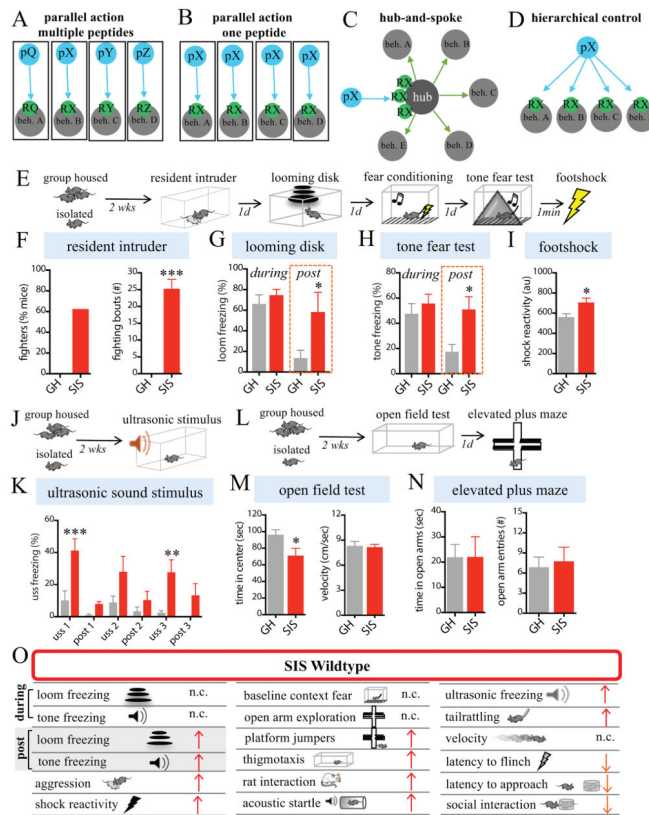
- Hatch A, Wiberg GS, Balazs T, Grice HC. Long-term isolation stress in rats. *Science*. 1963; 142:507–508. [PubMed: 14064449]
- Haubensak W, Kunwar PS, Cai H, Ciochi S, Wall NR, Ponnusamy R, Biag J, Dong HW, Deisseroth K, Callaway EM, et al. Genetic dissection of an amygdala microcircuit that gates conditioned fear. *Nature*. 2010; 468:270–276. [PubMed: 21068836]
- Kim JJ, DeCola JP, Landeira-Fernandez J, Fanselow MS. N-methyl-D-aspartate receptor antagonist APV blocks acquisition but not expression of fear conditioning. *Behavioral neuroscience*. 1991; 105:126–133. [PubMed: 1673846]
- Hawkley LC, Cole SW, Capitanio JP, Norman GJ, Cacioppo JT. Effects of social isolation on glucocorticoid regulation in social mammals. *Hormones and behavior*. 2012; 62:314–323. [PubMed: 22663934]
- Hilakivi LA, Ota M, GLR. Effect of Isolation on Brain Monoamines and the Behavior of Mice in Tests of Exploration, Locomotion, Anxiety and Behavioral Despair. *Pharmacology, biochemistry, and behavior*. 1989; 33:371–374.
- Holt-Lunstad J, Smith TB, Baker M, Harris T, Stephenson D. Loneliness and Social Isolation as Risk Factors for Mortality. *Perspectives on Psychological Science*. 2015; 10:227–237. [PubMed: 25910392]
- Holt-Lunstad J, Smith TB, Layton JB. Social relationships and mortality risk: a meta-analytic review. *PLoS medicine*. 2010; 7:e1000316. [PubMed: 20668659]
- Hong W, Kim DW, Anderson DJ. Antagonistic control of social versus repetitive self-grooming behaviors by separable amygdala neuronal subsets. *Cell*. 2014; 158:1348–1361. [PubMed: 25215491]
- Hong W, Kennedy A, Burgos-Artizzu XP, Zelikowsky M, Navonne SG, Perona P, Anderson DJ. Automated measurement of mouse social behaviors using depth sensing, video tracking, and machine learning. *Proceedings of the National Academy of Sciences of the United States of America*. 2015; 112:E5351–5360. [PubMed: 26354123]
- House JS, Landis KR, Umberson D. Social relationships and health. *Science*. 1988; 241:540–545. [PubMed: 3399889]
- Hsiao EY, McBride SW, Hsien S, Sharon G, Hyde ER, McCue T, Codelli JA, Chow J, Reisman SE, Petrosino JF, et al. Microbiota modulate behavioral and physiological abnormalities associated with neurodevelopmental disorders. *Cell*. 2013; 155:1451–1463. [PubMed: 24315484]
- Kash TL, Pleil KE, Marcinkiewicz CA, Lowery-Gionta EG, Crowley N, Mazzone C, Sugam J, Hardaway JA, McElligott ZA. Neuropeptide regulation of signaling and behavior in the BNST. *Molecules and cells*. 2015; 38:1–13. [PubMed: 25475545]
- Katz PS, Lillvis JL. Reconciling the deep homology of neuromodulation with the evolution of behavior. *Current opinion in neurobiology*. 2014; 29:39–47. [PubMed: 24878891]
- Katz RJ, Roth KA, Carroll BJ. Acute and chronic stress effects on open field activity in the rat: implications for a model of depression. *Neuroscience and biobehavioral reviews*. 1981; 5:247–251. [PubMed: 7196554]
- Kessler RC, Aguilar-Gaxiola S, Alonso J, Chatterji S, Lee S, Ormel J, Ustun TB, Wang PS. The global burden of mental disorders: an update from the WHO World Mental Health (WMH) surveys. *Epidemiologia e psichiatria sociale*. 2009; 18:23–33. [PubMed: 19378696]
- Kim J, Zhang X, Muralidhar S, LeBlanc SA, Tonegawa S. Basolateral to Central Amygdala Neural Circuits for Appetitive Behaviors. *Neuron*. 2017; 93:1464–1479. e1465. [PubMed: 28334609]
- Koch M. The neurobiology of startle. *Progress in neurobiology*. 1999; 59:107–128. [PubMed: 10463792]
- Koob GF. Corticotropin-releasing factor, norepinephrine, and stress. *Biological psychiatry*. 1999; 46:1167–1180. [PubMed: 10560023]
- Kormos V, Gaszner B. Role of neuropeptides in anxiety, stress, and depression: from animals to humans. *Neuropeptides*. 2013; 47:401–419. [PubMed: 24210138]
- Kunwar PS, Zelikowsky M, Remedios R, Cai H, Yilmaz M, Meister M, Anderson DJ. Ventromedial hypothalamic neurons control a defensive emotion state. *eLife*. 2015:4.
- LeDoux J. Rethinking the Emotional Brain. *Neuron*. 2012; 73:653–676. [PubMed: 22365542]

- Lee H, Kim DW, Remedios R, Anthony TE, Chang A, Madisen L, Zeng H, Anderson DJ. Scalable control of mounting and attack by Esr1+ neurons in the ventromedial hypothalamus. *Nature*. 2014; 509:627–632. [PubMed: 24739975]
- Lein ES, Hawrylycz MJ, Ao N, Ayres M, Bensinger A, Bernard A, Boe AF, Boguski MS, Brockway KS, Byrnes EJ, et al. Genome-wide atlas of gene expression in the adult mouse brain. *Nature*. 2007; 445:168–176. [PubMed: 17151600]
- Lu, A., Steiner, MA., Whittle, N., Vogl, AM., Walser, SM., Ableitner, M., Refojo, D., Ekker, M., Rubenstein, JL., Stalla, GK., Singewald, N., Holsboer, F., Wotjak, CT., Wurst, W., Deussing, JM. *Molecular psychiatry*. 2008. Conditional mouse mutants highlight mechanisms of corticotropin-releasing hormone effects on stress-coping behavior; p. 1028-1042.
- Madisen L, Zwingman TA, Sunkin SM, Oh SW, Zariwala HA, Gu H, Ng LL, Palmiter RD, Hawrylycz MJ, Jones AR, Lein ES, Zeng H. A robust and high-throughput Cre reporting and characterization system for the whole mouse brain. *Nature neuroscience*. 2010; 13:133–140. [PubMed: 20023653]
- Maggio JE. Tachykinins. *Annual review of neuroscience*. 1988; 11:13–28.
- Matsumoto K, Pinna G, Puia G, Guidotti A, Costa E. Social isolation stress-induced aggression in mice: a model to study the pharmacology of neurosteroidogenesis. *Stress*. 2005; 8:85–93. [PubMed: 16019600]
- Matthews GA, Nieh EH, Vander Weele CM, Halbert SA, Pradhan RV, Yosafat AS, Glober GF, Izadmehr EM, Thomas RE, Lacy GD, Wildes CP, Ungless MA, Tye KM. Dorsal Raphe Dopamine Neurons Represent the Experience of Social Isolation. *Cell*. 2016; 164:617–631. [PubMed: 26871628]
- McCall, JG., Al-Hasani, R., Siuda, ER., Hong, DY., Norris, AJ., Ford, CP., Bruchas, MR. *Neuron*. Elsevier Inc; 2015. CRH Engagement of the Locus Coeruleus Noradrenergic System Mediates Stress-Induced Anxiety; p. 605-620.
- McEwen BS, Bowles NP, Gray JD, Hill MN, Hunter RG, Karatsoreos IN, Nasca C. Mechanisms of stress in the brain. *Nature neuroscience*. 2015; 18:1353–1363. [PubMed: 26404710]
- Mongeau R, Miller GA, Chiang E, Anderson DJ. Neural correlates of competing fear behaviors evoked by an innately aversive stimulus. *The Journal of neuroscience : the official journal of the Society for Neuroscience*. 2003; 23:3855–3868. [PubMed: 12736356]
- Naito Y, Yoshimura J, Morishita S, Ui-Tei K. siDirect 2.0: updated software for designing functional siRNA with reduced seed-dependent off-target effect. *BMC bioinformatics*. 2009; 10:392. [PubMed: 19948054]
- Navarro VM. Interactions between kisspeptins and neurokinin B. *Advances in experimental medicine and biology*. 2013; 784:325–347. [PubMed: 23550013]
- Regev L, Neufeld-Cohen A, Tsoory M, Kuperman Y, Getselter D, Gil S, Chen A. Prolonged and site-specific over-expression of corticotropin-releasing factor reveals differential roles for extended amygdala nuclei in emotional regulation. *Molecular psychiatry*. 2011; 16:714–728. [PubMed: 20548294]
- Regev L, Tsoory M, Gil S, Chen A. Site-specific genetic manipulation of amygdala corticotropin-releasing factor reveals its imperative role in mediating behavioral response to challenge. *Biological psychiatry*. 2012; 71:317–326. [PubMed: 21783178]
- Remedios R, Kennedy A, Zelikowsky M, Grewe BF, Schnitzer MJ, Anderson DJ. Social behaviour shapes hypothalamic neural ensemble representations of conspecific sex. *Nature*. 2017 in press.
- Sapolsky RM. Why stress is bad for your brain. *Science*. 1996; 273:749–750. [PubMed: 8701325]
- Selye H. A syndrome produced by diverse nocuous agents. *Nature*. 1936:138.
- Shi L, Fatemi SH, Sidwell RW, Patterson PH. Maternal influenza infection causes marked behavioral and pharmacological changes in the offspring. *The Journal of neuroscience : the official journal of the Society for Neuroscience*. 2003; 23:297–302. [PubMed: 12514227]
- Sink KS, Walker DL, Freeman SM, Flandreau EI, Ressler KJ, Davis M. Effects of continuously enhanced corticotropin releasing factor expression within the bed nucleus of the stria terminalis on conditioned and unconditioned anxiety. *Molecular psychiatry*. 2012; 18:308–319. [PubMed: 22290119]
- Spooren W, Riemer C, Meltzer H. Opinion: NK3 receptor antagonists: the next generation of antipsychotics? *Nature reviews Drug discovery*. 2005; 4:967–975. [PubMed: 16341062]

- Taghert PH, Nitabach MN. Peptide neuromodulation in invertebrate model systems. *Neuron*. 2012; 76:82–97. [PubMed: 23040808]
- Tasic B, Menon V, Nguyen TN, Kim TK, Jarsky T, Yao Z, Levi B, Gray LT, Sorensen SA, Dolbeare T, Bertagnolli D, Goldy J, Shapovalova N, Parry S, Lee C, Smith K, Bernard A, Madisen L, Sunkin SM, Hawrylycz M, Koch C, Zeng H. Adult mouse cortical cell taxonomy revealed by single cell transcriptomics. *Nature neuroscience*. 2016; 19:335–346. [PubMed: 26727548]
- Thurmond JB. Technique for producing and measuring territorial aggression using laboratory mice. *Physiol Behav*. 1975; 14:879–881. [PubMed: 1237905]
- Thompson CL, Pathak SD, Jeromin A, Ng LL, MacPherson CR, Mortrud MT, Cusick A, Riley ZL, Sunkin SM, Bernard A, et al. Genomic anatomy of the hippocampus. *Neuron*. 2008; 60:1010–1021. [PubMed: 19109908]
- Toth M, Mikics E, Tulogdi A, Aliczki M, Haller J. Post-weaning social isolation induces abnormal forms of aggression in conjunction with increased glucocorticoid and autonomic stress responses. *Hormones and behavior*. 2011; 60:28–36. [PubMed: 21316368]
- Umberson D, Montez JK. Social relationships and health: a flashpoint for health policy. *Journal of health and social behavior*. 2010; 51(Suppl):S54–66. [PubMed: 20943583]
- Valzelli, L. Aggressive behavior induced by isolation. In: Garattini, S., Sigg, EB., editors. *Aggressive behavior*. Amsterdam, The Netherlands: Excerpta Media; 1969.
- Valzelli L. The “isolation syndrome” in mice. *Psychopharmacologia*. 1973; 31:305–320. [PubMed: 4582344]
- Walker DL, Miles LA, Davis M. Selective participation of the bed nucleus of the stria terminalis and CRF in sustained anxiety-like versus phasic fear-like responses. *Prog Neuropsychopharmacol Biol Psychiatry*. 2009; 33:1291–1308. [PubMed: 19595731]
- Wang L, Dankert H, Perona P, Anderson DJ. A common genetic target for environmental and heritable influences on aggressiveness in *Drosophila*. *Proceedings of the National Academy of Sciences of the United States of America*. 2008; 105:5657–5663. [PubMed: 18408154]
- Weiss IC, Pryce CR, Jongen-Rêlo AL, Nanz-Bahr NI, Feldon J. Effect of social isolation on stress-related behavioural and neuroendocrine state in the rat. *Behavioural brain research*. 2004; 152:279–295. [PubMed: 15196796]
- Witkin JM, Statnick MA, Rorick-Kehn LM, Pintar JE, Ansonoff M, Chen Y, Tucker RC, Ciccocioppo R. The biology of Nociceptin/Orphanin FQ (N/OFQ) related to obesity, stress, anxiety, mood, and drug dependence. *Pharmacology & therapeutics*. 2014; 141:283–299. [PubMed: 24189487]
- Yilmaz M, Meister M. Rapid innate defensive responses of mice to looming visual stimuli. *Current biology : CB*. 2013; 23:2011–2015. [PubMed: 24120636]
- Zelikowsky M, Hersman S, Chawla MK, Barnes CA, Fanselow MS. Neuronal ensembles in amygdala, hippocampus, and prefrontal cortex track differential components of contextual fear. *The Journal of neuroscience : the official journal of the Society for Neuroscience*. 2014; 34:8462–8466. [PubMed: 24948801]

**HIGHLIGHTS**

- Chronic social isolation stress (SIS) causes a pervasive change in brain state
- SIS broadly up-regulates expression of Tac2/NkB in multiple brain regions
- Tac2 up-regulation is necessary and sufficient for behavioral influences of SIS
- NkB acts locally in different brain areas to orchestrate behavioral effects of SIS ITI



significance ( $p > 0.05$ ). ANOVA's,  $F$  values,  $t$  values, as well as additional statistical information for this and subsequent figures can be found in Table S1. See related Figure S1.

Author Manuscript

Author Manuscript

Author Manuscript

Author Manuscript

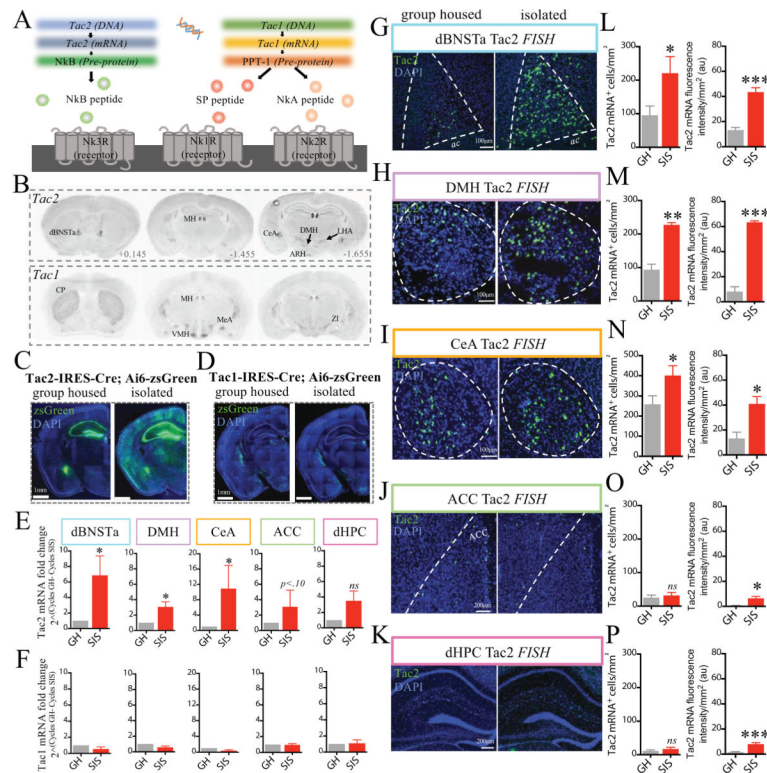


**Figure 2. SIS causes an increase in Tac2 expression**

(A) Illustration summarizing tachykinin ligand-receptor specificities.

(B) Tac2 (top panels) and Tac1 (bottom panels) mRNA expression (coronal sections) revealed by in situ hybridization (ISH) (data from Mouse Brain Atlas, Allen Institute of Brain Science; Tac2, Exp. 72339556; Tac1, Exp.1038). Abbreviations: dBNSTa, anterodorsal bed nucleus of the stria terminalis; MH, medial habenula; CeA, central amygdala; DMH, dorsomedial hypothalamus; ARH, arcuate nucleus; LHA, lateral hypothalamus; CP, caudate putamen; MeA, medial amygdala; VMH, ventral medial hypothalamus; ZI, zona incerta.

(C–D) Coronal sections of expression of zsGreen in GH vs. 2 week-isolated Tac2-IRES-Cre (C) or Tac1-IRES-Cre (D) mice crossed to Ai6 (zsGreen) Cre reporter mice.

(E–F) Quantification of Tac2 or Tac1 mRNAs by qRT-PCR in the indicated regions, hand-dissected from the brains of GH or SIS mice (n=4 mice/condition).

(G–K) Tac2 mRNA detected by FISH in GH or SIS mice in the indicated regions (n= 3–4 mice/condition, 1–4 sections/region/mouse); representative sections from each area are shown. Dashed lines indicate regions of interest (ROIs) used for quantification.

(L–P) Left, avg. number of Tac2 mRNA<sup>+</sup> cells/mm<sup>2</sup> in ROIs; Right, avg. fluorescence intensity/mm<sup>2</sup> in the regions shown in (I–M), respectively. Fold-increases in Tac2 mRNA fluorescence intensity are greater than increases in cell number, indicating an increase in expression level per cell.

See related Figure S2.

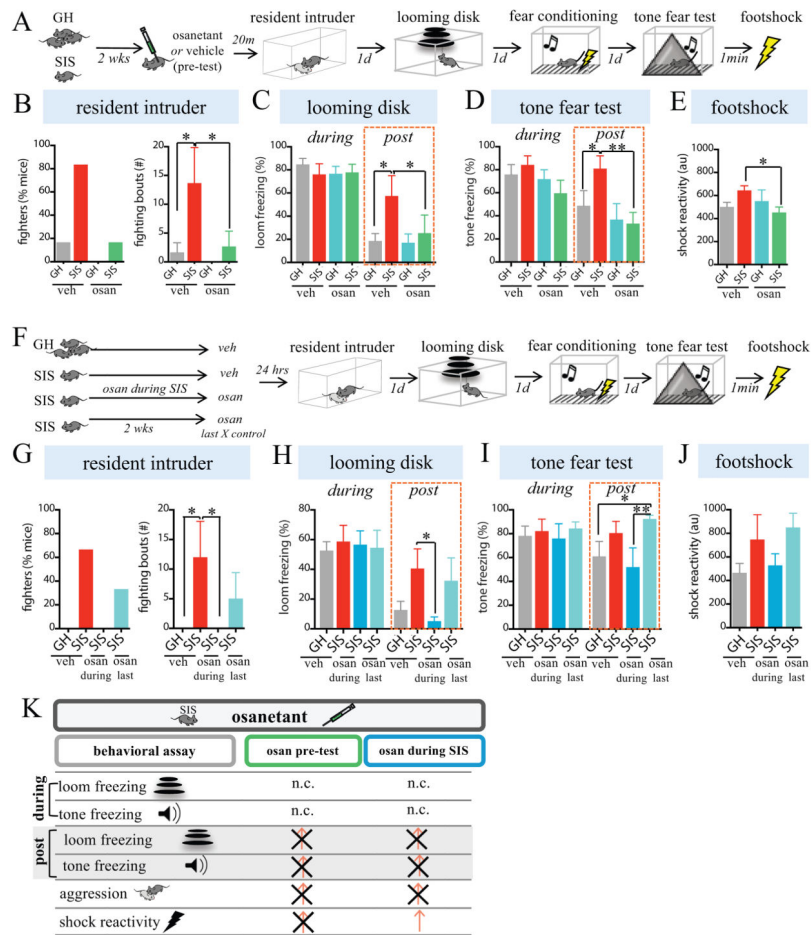


### Figure 3. Systemic Nk3R antagonism attenuates effects of SIS

(A) Experimental protocol. Following isolation, SIS or GH mice were injected (i.p.) with osanetant or vehicle and tested for the indicated behaviors (n=6 mice/condition).

(B–E) Osanetant blocked SIS-induced aggression (B), post-loom freezing (C), post-tone freezing (D), and increased shock reactivity (E).

(F) Experiment to test whether osanetant delivered daily during SIS can protect against its behavioral effects. “osan last” indicates an additional control group given just the last dose of osan 24 hours before testing to control for carry-over of the drug (n=6/condition).

(G–J) Effect of osanetant administered during SIS on (G) aggression, (H) post-loom freezing, (I) post-tone freezing. (J) Shock reactivity; a trend to protection (SIS-veh vs. osan during) was observed but did not reach our significance threshold ( $p > .05$ ).

(K) Summary of results. “osan pre-test” indicates osanetant was given 20 min prior to each assay (B–E) but not during SIS, “osan during SIS” indicates osanetant was given during SIS only (G–J), and not 20 min before each assay. Faint red arrows indicate original effects produced by SIS. Black X’s indicate SIS-induced effects that were blocked by the manipulation.

See related Figure S3.

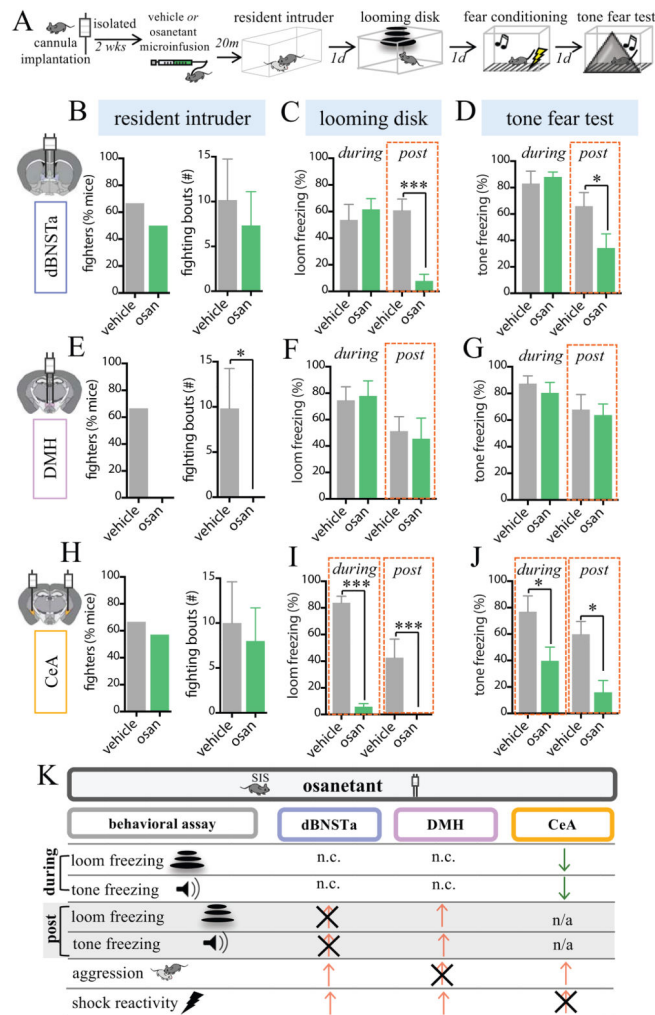


**Figure 4. Targeted NK3R antagonism in dBNSTa, DMH, or CeA attenuates different effects of SIS in a dissociable manner**

(A) Experimental protocol. Mice were implanted with bilateral cannulae in dBNSTa, DMH, or CeA, isolated, and given osanetant or vehicle microinfusions (300nl) 20 min before testing ( $n=6-7$ /condition).

(B–J) Effect of osanetant infusion into dBNSTa (B–D), DMH (E–G), or CeA (H–J) on indicated assays. Osanetant (green bars) selectively blocked persistent freezing in dBNSTa (“post”; C–D), aggression in DMH (E), and acute freezing in CeA (“during”; I–J).

(K) Summary of results. Notations as in Fig. 3K. n/a, not applicable (secondary to lack of freezing during stimulus). Green down-pointing arrows indicate manipulation-induced reduction in a behavior not altered by SIS.

See related Figure S4.

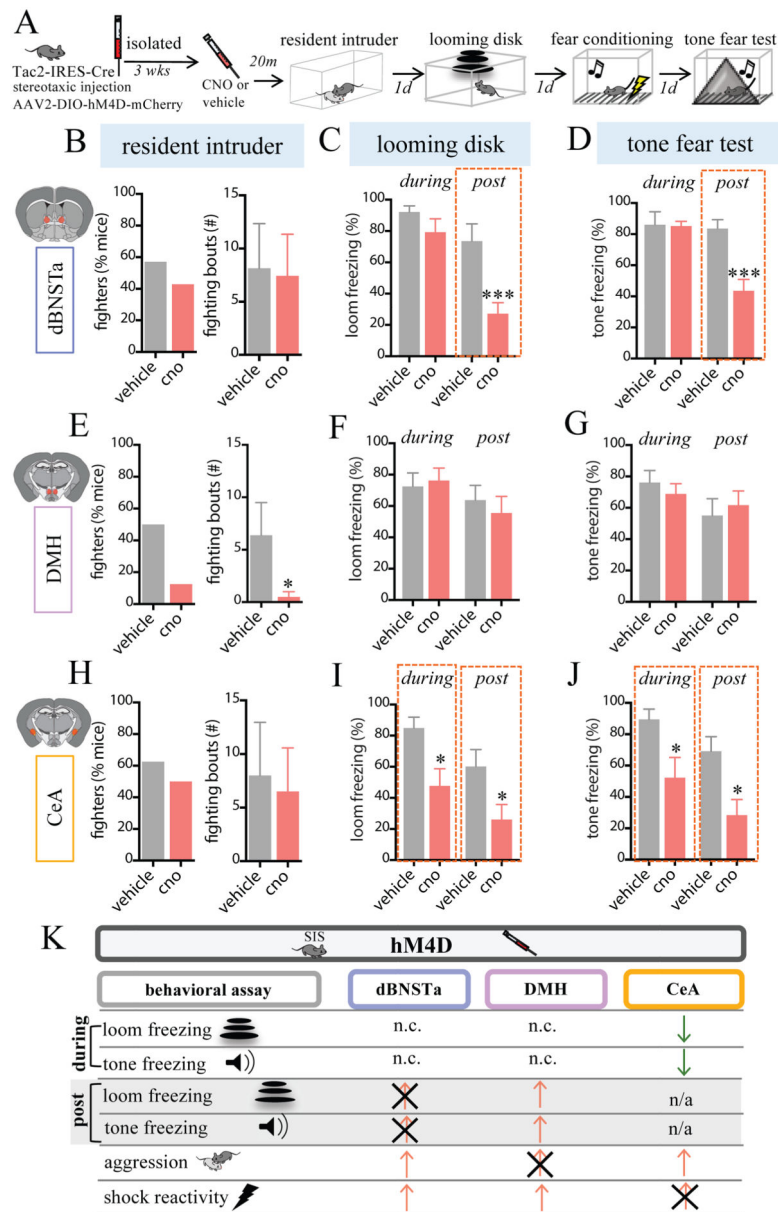


**Figure 5. Targeted chemogenetic silencing of Tac2<sup>+</sup> cells attenuates the effects of SIS**

(A) Experimental protocol. Tac2-Cre mice were bilaterally injected in the indicated regions with a Cre-dependent AAV expressing hM4DREADD-mCherry, isolated, and injected (i.p.) with CNO or vehicle prior to testing (n=7–8 mice/condition).

(B–J) Effect of vehicle or CNO on mice expressing Tac2-hM4DREADD in dBNSTa (B–D), DMH (E–G), or CeA (H–J) on indicated assays. CNO blocked persistent freezing in dBNSTa (“post”; C–D), aggression in DMH (E), and acute freezing in CeA (“during”; I–J).

(K) Summary of results. Notations as in Fig. 4K. CNO had no effect in mCherry-expressing mice (Fig. S5E).

See related Figure S5.

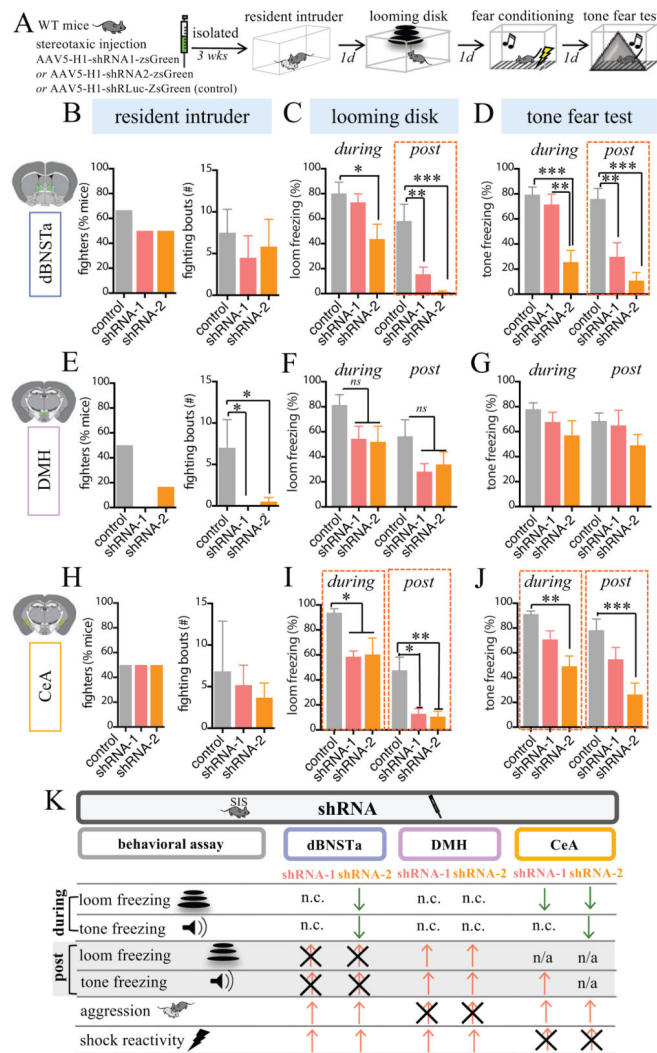


**Figure 6. Targeted knockdown of Tac2 attenuates the effects of SIS**

(A) Experimental protocol. 3 weeks prior to testing, wildtype (WT) mice were injected with an AAV expressing shRNA-zsGreen for specific knockdown of Tac2 (shRNA-1 or shRNA-2), or with an shRNA virus targeting the *luciferase* gene (control) (n=6–7/mice condition), and maintained in isolation until testing.

(B–J) Effect of shRNA's in dBNSTa (B–D); DMH (E–G), or CeA (H–J) on indicated assays. shRNA-1 (red bars) blocked persistent freezing in dBNSTa (“post”; C–D); aggression in DMH (E) and freezing in CeA (I–J). shRNA-2 (orange bars) yielded similar effects but additionally reduced acute freezing in dBNSTa (“during”; C, D).

(K) Summary of results. The effects of shRNA-1 (left column) and shRNA-2 (right column) are presented for each region.

See related Figure S6.

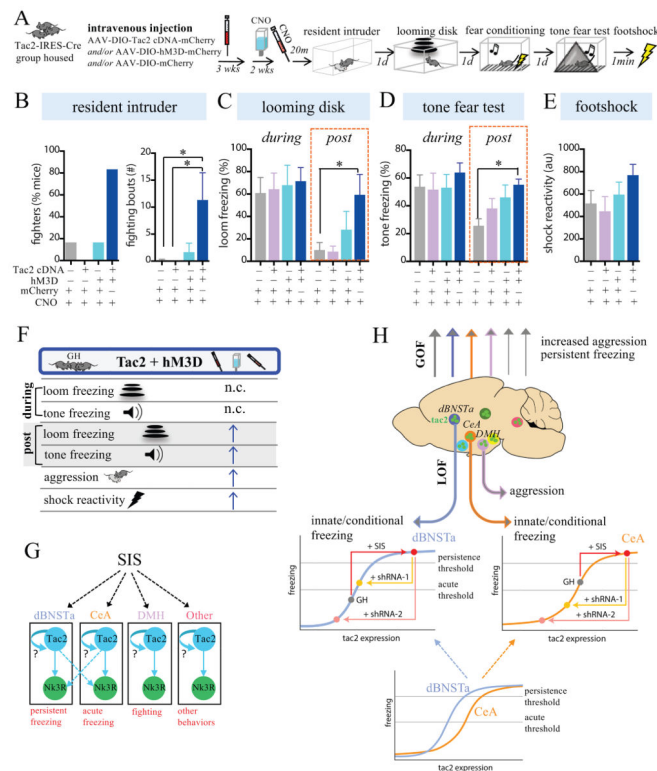


**Figure 7. Activation of Tac2<sup>+</sup> neurons plus Tac2 overexpression mimics the effects of SIS in GH Mice**

(A) Experimental protocol. GH Tac2-IRES-Cre mice were intravenously injected with Cre-dependent, human Synapsin I promoter-driven, AAV-PHP.B serotyped viruses expressing the chemogenetic activator hM3DREADD, a Tac2 cDNA, both, or just mCherry (controls). Mice remained group housed (5 weeks) with CNO-spiked drinking water provided during the final 2 weeks (for hM3DREADD activation). Mice received an injection of CNO (i.p.) 20 min prior to each assay (n=6 mice/condition).

(B–E) Effect of each manipulation on the indicated assays. All animals were treated with CNO and received the same total amount of virus. Only mice receiving both the hM3DREADD and Tac2 cDNA viruses showed an “SIS-like” phenotype (dark blue bars), including increased aggression (B), post loom freezing (C), and post-tone freezing (D). (E) Reactivity to the footshock.

(F) Summary of results. Blue arrows indicate effects of perturbations to generate SIS-like effects.

(G) Schematic illustrating how Tac2 and its receptor (Nk3R) may control SIS-induced behavior.

(H) (*Upper*) Illustration summarizing LOF and GOF effects on behavior. (*Lower*) Model graphs showing how different thresholds for acute vs. persistent freezing, and different dose-dependencies of freezing on Tac2 levels in dBNSTa vs. CeA (bottom graph), could explain the differential effects of shRNA -1 (weaker) and -2 (stronger; upper graphs) in the two regions (see Fig. 6). The model also illustrates how an increase in Tac2 levels caused by SIS (red line) could convert acute (CeA-dependent) to persistent (dBNSTa-dependent) freezing.

Gray dot, baseline levels of Tac2 in GH mice are higher in CeA than in dBNSTa, based on *FISH* data (Fig. 2L, N).  
See related Figure S7.

Author Manuscript

Author Manuscript

Author Manuscript

Author Manuscript